Assessing the spatiotemporal variation of phytoplankton biomass in Nandoni reservoir in the Vhembe District (South Africa) using LANDSAT satellite imagery

by

Fulufhelo Faith Muthivhi

Student number: 11530643

Thesis submitted in fulfilment of the requirements for the degree of Masters in Environmental Sciences in the Department of Geography and Environmental Sciences, University of Venda

Supervisors: Dr T. Dalu, Mr F. Dondofema, Dr M.J. Mokgoebo

December 2021

ABSTRACT

Chlorophyll–*a* (chl–*a*) is an optical active compound used as proxy for phytoplankton biomass to determine the trophic state of the aquatic ecosystem. Traditional approaches for monitoring aquatic system are time consuming, expensive, and non–continuous, therefore, Remote Sensing technologies are qualitative for monitoring the status for water quality in large scale and low cost. The aim of this study was to assess the spatial and temporal variation of phytoplankton biomass in Nandoni reservoir, Limpopo to examine the relationship that exist between the physico–chemical variables and chl–*a* concentration using readily available Landsat multispectral images. Multispectral resolution of (30 m) Landsat 7 ETM+ and Landsat 8 OLI images for June to December 2008 to 2020 were used to derive the distribution of chl–*a* concentration. The spatial distribution of chl–a concentration in wet and dry season of these years was obtained. By using regression techniques, *in situ* measured chl–*a* was related to construct and validate Landsat predicted chl–*a* to determine the distribution of chl–*a* in the reservoir. The results indicate that Landsat derived chl–*a* was similar with the observed measured chlorophyll–*a* ($R^2 = 0.91$). There was a negative significant correlation among Land Use and Land Cover with water quality ($P > 0.05$). Using permutational multivariate analysis of variance (PERMANOVA) analysis, there was significant differences for chl–*a* concentration in sites, seasons, and zones. There was positive significant correlation observed on water temperature with strong negative significant with salinity and TDS. A strong perfect linear association among predicted *vs* measured chl–*a* were found. Chlorophyll–*a* concentration in Nandoni reservoir was derived using Landsat remote sensing images, suggesting that Landsat sensor is suitable for monitoring small reservoir in a short timescale. Remote sensing techniques can be used to control the development of an early warning system of this study and other reservoirs.

TABLE OF CONTENTS

ACKNOWLEDGEMENTS

My deepest gratitude goes to God Almighty who has provided all that was needed to complete my project. There was never a lack or want. Throughout this study He took care of everything that would have stopped me in my tracks and strengthened me through my most difficult times.

I would like to thank my supervisors Dr T. Dalu, Mr F. Dondofema, and Dr M.J Mokgoebo for their patient, guidance, encouragement, and willingness to give their time so generously throughout this project has been very much appreciated. I would like to extend my deepest gratitude to Mr F.L. Munyai who worked very hard and showed much support and patience during my research.

My heartfelt gratitude goes to my beloved family for not giving up on me, for their support and effort. I could not have done it without my dad, mother, who supported me emotionally and financially. My beloved siblings, your love, and support has meant the world to me. I always knew you wanted the best out of me. My son Onndwela, you are my inspiration to achieve greatness. Without you I would not be where I am today.

DEDICATION

I would like to dedicate this work to my son and family who supported me throughout my studies. You have made me stronger, better, and more fulfilled than I could ever imagine.

DECLARATION

I declare that **"Assessing the spatiotemporal variation of phytoplankton biomass in Nandoni reservoir in the Vhembe District (South Africa) using Landsat satellite imagery"** is my own work. All other sources, used or quoted, have been indicated and acknowledged by means of complete references. This work has not been submitted for a degree at another university.

Fulufhelo Faith Muthivhi

Date: 10 December 2021

CHAPTER ONE: INTRODUCTION

1.1 Introduction

Phytoplankton are microscopic plants that are free floating in the freshwater, brackish and/or marine ecosystems, and are autotrophic organisms that produce food through photosynthesis. Therefore, phytoplankton plays an important role in producing food in aquatic ecosystems (Berglund *et al*. 2007). Phytoplankton contain chlorophyll–*a* which assist them to capture light energy and utilise the energy during photosynthesis to turn it into carbohydrates and oxygen. Chlorophyll–*a* is a colour pigment found primarily in plant taxa such as phytoplankton, the biomass of phytoplankton can be determined by examining the concentration of chlorophyll–*a* in water bodies (Gregor and Marsalek, 2004; Bowes *et al*. 2012).

The chlorophyll–*a* concentration levels indicate the abundance of phytoplankton and possible the level of primary production in aquatic ecosystems (Gurung *et al*. 2006). Therefore, elevated chlorophyll–*a* concentrations are generally associated with a change in the trophic status of a water body and are traditionally associated with a reduction in water quality and lowered biodiversity, which destabilizes ecosystem services and functioning (Dalu *et al*. 2013). Phytoplankton abundances in reservoirs are experience seasonal changes due to nutrient variability between seasons (Paulett *et al*. 2011). Physical factors of the reservoir greatly influence phytoplankton structure, for examples water flow fluctuation in reservoirs allows for the exchange and recruitment of species (Moura *et al*. 2013).

Phytoplankton growth rate depends on factors such as water temperature, water depth, wind, and a variety of predators that graze on them (Margalef, 1958). Due to natural and anthropogenic disturbance occurring in the waterbodies, different water quality parameters present in the reservoirs are likely to be affected by these activities. Chemical parameters include pH, nitrogen, chemical dissolved oxygen (COD), and dissolved oxygen (DO), biological parameters include algae and bacteria, and physical parameters include temperature, turbidity, and electrical conductivity (EC) (Supp and Ernest, 2014). The main processes that structure phytoplankton in reservoirs differ in space and time due to the changes in chemical and physical parameters creates a vital influence on the trophic change of aquatic ecosystems (Kimmel *et al*. 1990; Li *et al*. 2018). These normally take place as water bodies undergo a gradual process of nutrient enrichment as the reservoirs ages (Supp and Ernest, 2014; Tijare *et al.* 2015). The activities taking place in reservoirs leading to phytoplankton production can be determined by the reservoir ages. The source of nutrients such as nitrate and ammonia, include urban developments, raw sewage effluent, fertilisers, and livestock (Lehman, 2014). Water quality in reservoirs worldwide faces various problems emanating from anthropogenic activities (El–Serehy *et al*. 2018).

Anthropogenic activities have accelerated the rate of eutrophication in aquatic ecosystems through point source discharge (partially treated wastewater effluents, raw sewage, treated or untreated industrial effluent) and non–point (fertiliser application, land clearing, farming). Nutrient loading (i.e., nitrogen, phosphorus) into aquatic environments lead to dramatic consequences for both fisheries, domestic and industrial water uses. Nutrient enrichment in aquatic ecosystems has becoming an area of increasing concern particularly in lakes, rivers, wetland, and reservoirs worldwide (Smith *et al*. 2006). Nutrients exported directly or indirectly into aquatic ecosystems can lead to rapid and extreme eutrophication. Eutrophication can lead a wide range of positive and negative effects on aquatic ecosystems. The relative nutrient concentration varies spatially and temporally. Aquatic ecosystems that are in landscapes dominated by nutrient–rich and fluvial sediments may naturally, become eutrophied even in the absence of anthropogenic activities. This normally takes place as aquatic ecosystems undergo a gradual process of nutrient enrichment as the reservoir age and this process is termed natural eutrophication (Reynolds, 2006; Mouillot *et al*. 2013; Supp and Ernest, 2014).

The flow of water in aquatic ecosystems serve as the main hydrological factor that influence phytoplankton structure, due to its ability to act upon a variety of environmental factors such as turbidity, turbulence, and residence time which may alter community dynamics (Kenderov *et al*. 2014). The quantity and size of phytoplankton biomass strongly influence the trophic level in reservoirs. Water in a reservoir is prone to longitudinal and vertical movement created by the climatic forces (Souza *et al*. 2016). The relationship between phytoplankton biomass and nutrients is likely to show a complex situation in tropical aquatic ecosystems, due to the influence of light, hydrology and grazing which may reduce phytoplankton production and biomass s (Rangel *et al*. 2012). Temporal changes in rainfall, land–use, use of reservoirs, hydrology, and morphology can affect the trophic state of the reservoirs (An and Kim, 2003). Reservoirs also experience environmental changes due to land–use shifts, geology, climate change, catchment hydrology, and species invasion (Jeppensen *et al*. 2015; Haliuc *et al.* 2020).

Remote sensing is a technology that be used to detect and monitor water quality variables using satellites, where satellite create images consisting of several spectral band sensors (Danoedoro, 2012). Remote sensing techniques can be used to monitor the spatio–temporal dynamics of reservoirs and other aquatic ecosystems to predict ecological changes and prepare for the consequences of these changes (Dall'Olmo *et al*. 2005). The surface reflectance of the water body is measured using remote sensing to determine the chlorophyll–*a* concentration. The use of remote sensing has the potential to provide synoptic estimates of chlorophyll–*a* concentration in aquatic environments (Harvey *et al*. 2015). Chlorophyll–*a* can also be employed as a proxy to estimate primary production of aquatic ecosystems (Olmanson *et al*. 2005; Matthews *et al*. 2010).

The estimation and mapping water quality variables is important in water management and planning, and therefore water quality information necessary to comprehend the current conditions and future trends of natural aquatic ecosystems (McGrane *et al*. 2016). The factors that can alter the spectral reflectance properties of water can be identified and quantified through hyper–spectral and multispectral remote sensing techniques (Melin *et al*. 2015). Mapping of water quality can be done through remote sensing (RS) and geographic information systems (GIS) to identify the types of variability that exist in the aquatic ecosystems (Schiebe *et al*. 2000).

Remote sensing techniques can be used to detect and map water quality variables and to help in decision–making by various organisations for future planning of water resource allocation, as well as agricultural and industrial impacts (Dube *et al*. 2015). This is because remote sensing techniques can be used to map and estimate water quality parameters of the entire aquatic waterbody. However, the measurement techniques of water quality variables can be measured at specific points where samples are collected (Gholizadeh *et al*. 2016). The advantage of remote sensing is the continuous monitoring of the entire aquatic waterbody and help with the refining and testing of biological models by serving as a link between laboratory measurements and the real time data (Dube *et al*. 2015).

Remote sensing methods have been used widely to detect and map various water physical parameters (Lavery *et al*. 1993; Gitelson *et al*. 2007). With its high spatial and spectral resolution, remote sensing can be useful in detecting and mapping water quality variables of large water bodies (Ekercin, 2007; Blondeau–Patissier *et al*. 2014). Remote sensing of water quality is regarded as promising and cost effective. There are free readily available remote sensing data such as Landsat 7 ETM+ and 8 OLI that often provide a synoptic and constituent view of aquatic ecosystem parameters (Olmanson *et al*. 2015).

Water quality classification forms part of supervised classification of remote sensing images which allows for the selection of sample pixels in an image that are representative of specific classes and then direct the image processing software as the classification of all other pixel in the image (Blakey et al. 2015). Most chlorophyll–*a* are based on simple blue to green band of ratio unlike for the aquatic ecosystems where a simple band ratio is not suitable for the covering water parameters. But for inland waters that are rich in biomass where phytoplankton dominates the optical properties where simple band ratio can be utilised (Toming *et al*. 2016). The bands in the green to near infrared (NIR) region are more effective for retrieving chlorophyll–*a* concentration (Rodriguez *et al*. 2020).

1.2 Problem statement

Phytoplankton biomass in reservoirs plays a significant role. However, the spatio–temporal variation in their biomass which can either be seasonally or annually, and it is often affected by anthropogenic activities such as agricultural development, urbanisation, and industrialisation which can introduce excessive nutrients into the ecosystem and accelerate the rate of eutrophication (Freeman *et al*. 2015). However, under favourable environmental conditions, the excessive nutrient enrichment (nitrogen and phosphorus) deposited into the reservoirs can trigger a rapid reproduction and growth of microscopic phytoplankton. The abrupt changes of phytoplankton productivity in reservoirs due to seasonal changes and their spatial location may lead to serious environmental problems such as low dissolved oxygen, death of aquatic organisms (e.g., fish), and decrease in ecological diversity (Kuang *et al*. 2005). The need therefore arises that phytoplankton biomass production in reservoirs be further investigated to determine whether the location of reservoirs and seasonal changes affect biomass composition and the effects on the aquatic ecosystem functioning.

Phytoplankton biomass is the base foundation of the aquatic food webs. They are primary producers that play a vital role of feeding every species from microscopic zooplankton to large vertebrate species (Isari *et al*. 2013). It is important to study how variations in chlorophyll–*a* changes seasonally and temporally in lentic environments for the better understanding of aquatic ecosystem functioning during different times of the year and in different environmental locations. This research will shed more light on the understanding of aquatic processes, and this will help to formulate better water quality management strategies for domestic, agricultural, and industrial use. Many studies on phytoplankton focused mainly on their productivity and largely on chlorophyll concentrations in water, as well as their role in photosynthesis of aquatic environments.

1.3 Research aim and objectives

1.3.1 Aim

To assess the spatial and temporal variation of phytoplankton biomass (i.e., chlorophyll–*a* concentration as a proxy) in Nandoni reservoir.

1.3.2 Objectives

- To examine water quality parameters of the reservoir and assess their relationship with phytoplankton biomass.

- To map spatio–temporal variation of phytoplankton biomass using remote satellite imagery across seasons and years

1.5 Hypotheses

- Remote sensing coupled with in situ measurements accurately predict chl–*a* fluctuation within tropical water bodies.
- Remote sensing and in situ measurements have little accuracy within the tropical water bodies.

CHAPTER TWO: LITERATURE REVIEW

2.1 Introduction

Bellinger *et al.* (2000) define phytoplankton as microscopic algae usually occurring in unicellular forms and are mostly photosynthetic. It is also an essential component of aquatic food chain. Phytoplankton has been used as an indicator of water quality. Phytoplankton plays a crucial role in regulating carbon concentration in the atmosphere. Given their short life span, they also respond swiftly to environmental changes such as temperature. Algae are photosynthetic eukaryotes that are single–celled, colonial, or multicellular. Some multicellular members are grouped into two main Empires or Domains (Prokaryota and Eukaryota) and then further down into multiple Kingdoms (e.g., Plantae), Supergroups, Divisions, etc. mainly in the Eukaryota Domain: Phylum Rhodophyta (red algae), Class Phaeophycea (brown algae) and Phyla Chlorophyta and Charophyta (green algae) (Collins *et al*. 2000). There are two main dominant types of phytoplankton species, which are diatoms and dinoflagellates. Diatoms are a single celled algal that live in a house which is made of glass. They are the only organisms on the planet characterised with cell walls which are composed of transparent, opaline silica structure. Diatoms have light absorbing molecules (chlorophyll–*a*) that assimilate solar energy and convert it into chemical energy through photosynthesis (Katsiapi *et al*. 2011). Phytoplankton species are mainly controlled by temperature, sunshine hours, nutrients, salts, water level and predation intensity. Previous research revealed that N and P are the main nutrients that limit the growth of phytoplankton in aquatic ecosystems (Xu *et al*. 2015; Yang *et al.* 2016, 2017).

2.2 Reservoir

Allan *et al*. (2006) defines a reservoir as an artificial place where water is stored and collected for multipurpose such as irrigation use, for domestic purpose, recreational, and fishery development. Reservoirs play a crucial role in the flood regulation by storing water and reducing flood risks (Danz *et al.* 2007). Reservoirs are important not only for electrical power generation but also for their multiple roles such as water supply, flood control, and navigation (Straskraba and Tundaris, 2013). Seasonal cooling together with other physical factors that occur daily in a reservoir combined with the mixing caused by wind leads to seasonal stratification (Wetzel, 2009). Low water velocities limit sediment suspension of the fine particles, leading to a more developed planktonic community. Anoxic conditions develop when organic matter settles into unmixed deep water when microbial consumption of DO takes place (Wetzel, 2001).

Understanding of phytoplankton dynamics in reservoirs can also be beneficial in evaluating the resilience standing water ecosystem, which can lead to a remarkable change of the limnological conditions that happens relatively in a short period. Phytoplankton in river channels is affected by cumulative effects of reservoirs in catchment basins by significantly blocking nutrient flow. Lentic aquatic habitats are formed by impoundment of rivers, and this makes phytoplankton to become the main primary producers of the pelagic zone by influencing the whole aquatic food web of newly created lentic ecosystems (Reynolds, 2006).

2.3 Seasonality and phytoplankton variation

Anthropogenic activities and climate change worldwide compromises the freshwater aquatic environments, especially shallow lakes and reservoirs (Jeppesen *et al*. 2014). Seasonal rainfall variation can change the amount of water stored in the reservoirs and other environmental variables such as turbidity, oxygen, and nutrients contents in the water column (Chaves *et al*. 2013; Mosley *et al*. 2015; Santos *et al*. 2017). Seasonal changes in phytoplankton population typically rely on seasonal variation of atmospheric physical factors, nutrient concentration, and biotic factors. Changes in climate and eutrophication rates strongly affect the aquatic ecosystems in shallow reservoirs (Sommer et al. 1986; Hong *et al*. 2014).

Reservoirs have two alternate key stable states in temperate environments, one in clear water and low phytoplankton biomass and other with turbid water (Carmignani *et al*. 2017). These seasonal changes have a major effect on the composition and structure of phytoplankton communities which are dominated by cyanobacteria and chlorophytes (Chakraborty *et al*. 2015). Variations in temperature and other environmental factors in subtropical regions can cause predictable changes in the phytoplankton composition in aquatic ecosystems (Grover and Chrzanowsli, 2006). Tropical areas, on the other hand, show little annual variation in temperature and successive shifts in the phytoplankton populations that are the products of seasonal rainfall trends, with various phytoplankton taxa in the wet and dry seasons (Ibanez, 1998; Enio, 2006).

Water level fluctuations have a significant consequence in reservoirs and other habitats and are a key factor for controlling phytoplankton biomass and species diversity, evenness, and community change in the reservoirs. Various phytoplankton groups respond to different changes in water level changes in the reservoirs (Naselli–Flores and Barone, 1997; Donagh *et al.* 2009; Arfi, 2005; Cott *et al*. 2008). Changes in water level can affect phytoplankton biomass and species composition in reservoir ecosystem (Naselli–Flores and Barone, 1997; Donagh *et al*. 2009).

2.4 Spatial location and phytoplankton variation

Spatial changes in the aquatic community structure occur due to a variety of factors present at different scales, especially within the tropical regions (Fonseca and Bicudo, 2008; Becker *et al.* 2009; Yang *et al.* 2018). Species composition and biomass of organisms is influenced by physical (e.g., light availability and mixing regime) and chemical factors (e.g., nutrient concentrations) that explain the longitudinal reservoir gradients (Thornton *et al.* 1998). Phytoplankton occurrence and development varies with season and can be attributed to factors such as rainfall patterns, light intensity, and temperature (DWAF, 2002).

Phytoplankton spatial heterogeneity could be decreased by the mass effect in spatially related aquatic environments such as streams and reservoirs. Therefore, strong species dispersal is promoted by water flow events. Reservoirs are extremely heterogeneous structures characterised by a range of habitats in the ecosystem with different environmental conditions (Kimmel *et al.* 1990). Therefore, the morphological and hydrological complexity may serve as an effective model for studying the relative importance of both environmental filtering (which should promote species sorting) and water flow (which should support mass effect) as a driving force of phytoplankton spatial distribution (Chorus and Bartram, 2002).

2.5 Age of catchment and phytoplankton

Population growth and development play an important role in the natural environment and this can be affected by human activities (Halpern et al. 2008). Human activities such as industrial wastewater, human water consumption increases, domestic sewage overflows and agricultural water withdrawal and fertilisers are impacting aquatic ecosystems within the aquatic ecosystems which impact reservoirs. Therefore, all these activities can lead to an increase of eutrophication in the reservoirs (Eom *et al*. 2017; Lv *et al.* 2014; Zhao *et al*. 2018a).

Reservoirs are water bodies that have a slow flow rate, low self–purification, and long water residence time. Therefore, nutrients are more likely to accumulate and create an environment that is conducive to phytoplankton (Toporowska *et al*. 2018). According to Dodds (2009), the water quality of reservoirs shifts markedly in chemical and physical characteristics. These changes are beneficial but there are many harmful changes that take place particularly during the early years that are dependent on reservoir's initial filling. These changes may reduce water quality directly or indirectly by encouraging rapid growth of phytoplankton in the aquatic environments (Smith *et al*. 2008).

Human activities have become the dominant negative factor affecting the aquatic environments worldwide and this has resulted in the water quality deterioration. Poor water quality can lead to many issues that can lead to deaths of many aquatic animals and seriously impacting the natural environment. Phytoplankton blooms can lead to large–scale reproduction of phytoplankton under suitable environment that can change dissolved oxygen (DO) concentration in the reservoir (O'Boyle *et al.* 2016). Furthermore, phytoplankton produces biotoxins such as microcystin that may pose serious health risks to humans, livestock, and safety of water consumption. All these water quality issues may result in large economic impacts such as increased water treatment costs and reduced tourism (Tollefson, 2018).

2.6 Physio–chemical variables and their relationship to phytoplankton community structure

The rapid increase of phytoplankton biomass and their production in reservoirs are often associated with environmental parameters (Oberholster *et al*. 2003). The physical water quality parameters include temperature, pH, salinity, electrical conductivity, total dissolved solids, and dissolved oxygen, while chemical parameters include nitrogen and phosphorus, ammonia, nitrate, and nitrite.

2.6.1 Temperature

Phytoplankton biomass favours the hot environment because their survival is impacted in cold environmental conditions. It is well known that phytoplankton prefers higher temperatures for survival ranging between 26 °C and 35 °C (Robarts and Zohary, 1987). As a major factor in the phytoplankton growth in freshwater bodies, high temperatures due to climate change have also been noted to lead to changes in community structure (Paul, 2008). Water temperature is also essential because phytoplankton growth rates are highly affected by water temperature. Phytoplankton is affected by water temperature directly by impacting the physiology and metabolic rates, and indirectly by its aquatic growth environment (Naselli–Flores *et al*. 2020). Phytoplankton can grow much faster in warmer waters than in cold waters. Increased water temperatures associated with global climate change are also likely to trigger phytoplankton shifts. Water temperature also influences the viscosity and water density, thus directly influencing the rate of sinking of small, suspended particles such as phytoplankton (Oberholster *et al*. 2013).

Phytoplankton biomass of reservoir in warmer tropical climate shares a biological unit which present the patterns of seasonal variation, in both cooler and warmer climates (Roelke *et al*. 2004). As global temperature increases, this tends to change the seasonality and precipitation around the reservoirs (IPCC, 2013). According to Moss *et al*. (2011), temperature will increase significantly, and this will affect water availability, quality, agricultural production and economies, and ecosystems.

2.6.2 pH

Phytoplankton finds their optimal growing conditions between 7.4 and 8.0 pH range. Phytoplankton can adapt in acidic surroundings, but their rate of development is impacted as their surrounding environment becomes more acidic (Rai and Rajashekar, 2014). Phytoplankton abundance increases in reservoirs when the pH is lowered, however, the phytoplankton abundance is expected to decrease when the pH is increased. Phytoplankton biomass is tolerant to pH, but when the water is more alkaline, this can reduce their growth as this was noted when pH exceeds 9.5 (Pendersen, 2003). Studies have shown that water contaminated generally have high pH which have negative effects on phytoplankton abundances (Leo and Dekkar, 2000).

2.6.3 Oxidation reduction potential (ORP)

Oxidation reduction potential measures the potential of lakes to purify itself or break down waste products. Phytoplankton usually grow within the range of 200 to 250 mV. Therefore, the higher the ORP value the healthier the reservoir, and there is lots of oxygen present in the water (Horne and Goldman 1994). ORP is measured in addition to dissolved oxygen because ORP can provide information on water quality and the degree of pollution in the water. Studies have shown that ORP depend on the amount of dissolve oxygen in the water as well as other elements that function similar to ORP. Additionally, when ORP is low, dissolve oxygen is low, this can be resulted because of sewage input and anthropogenic activities closer to the shoreline (Lopez et al., 2008).

2.6.4 Total dissolved solids and electrical conductivity (EC)

Total dissolved solids (TDS) occur naturally in aquatic ecosystems and also as a result of human activities. The TDS may come from a variety of natural and human–made sources. For example, mineral springs have high total dissolved solids due to high salt content from underground rocks. Human activities such as agricultural pesticides and urban runoff may bring excessive minerals to water bodies (Stensel, 2004). The TDS is also an important water chemical parameter primarily indicating the existence of different minerals including, ammonia, nitrate, nitrite, phosphate, alkaline, acids in dissolved forms (Rahman *et al.* 2012). The concentration of TDS in water has been one of the important features in water quality with values ranging from 0 to 250 mg/L (Dallas and Day (2004). Most freshwater bodies have conductivity values ranging from 1 to 100 µS/cm (Chapman and Kimstach, 1996). According to South African domestic water quality guidelines (DWAF, 1996b), there are no reports of health, aesthetic and/or therapeutic risk associated with conductivity ranging from 0 to 70 µS/cm.

2.6.5 Salinity

Salinity is a total inorganic ion concentration and essential environmental factor that influence species growth such as algae in the water ecosystem. Salinity has been confirmed as a strong determinant of phytoplankton by demonstrating the importance of nutrients supply Galloway and Winder (2015). Salinity concentrations in estuaries vary spatially and temporally, reflecting to relative inputs from the watershed and tidal water intrusion. Salinity has been suggested as a controlling factor of phytoplankton growth in freshwater (Baek *et al*. 2015). Salinity has been linked to phytoplankton diversity within the water ecosystem. Increased salinity reduces the rate of net carbon fixation in estuaries (Moisander *et al*. 2015). The tolerance of salinity determines how long phytoplankton will survive in tropical fresh water/marine ecosystem. Phytoplankton tolerate ranges of salinity values exceeding 7.5 PSU.

2.6.6 Resistivity

Formation water is the free water which supplies the energy for the water drive in reservoirs; and its resistivity is variable depending on the salinity, temperature and whether or not the formation contains hydrocarbons (Ushie, 2001). The electrical resistivity of a material is a number describing how much that material resists the flow of electricity. Resistivity is measured in units of ohm meters (Ω m). If electricity can flow easily through a material, that material has low resistivity. If electricity has great difficulty flowing through a material, that material has high resistivity (Heaney, 2003). The electrical resistivity contrasts that exist across interfaces of lithologic units in the subsurface are used to delineate discrete geoelectric layers and identify aquiferous or non–aquiferous layers (Aweto, 2013).

2.7 Remote sensing and water quality

Pettorelli (2016) defined remote sensing as a process of detecting and monitoring the physical characteristics of an area by measuring its reflected and emitted radiation at a distance. Remote sensing can provide water quality data for thousand reservoirs with high spatial and temporal resolution (Brando and Dekker, 2003). The assessment of environmental issues is supported by remote sensing through improving water quality and detecting phytoplankton biomass (Arief, 2017). The use of remote sensing to monitor the water quality is considered promising and less expensive (Vapnik, 2000).

Remote sensing tool provides spatial and temporal variation of the surface water quality parameters that are not readily accessible from in situ measurements, by enabling the landscape to be monitored accurately and efficiently, identifying, and quantifying parameters and problems of water quality (Oppelt, 2016). According to Matthews (2011) and Dornhofer and

Oppelt (2016), remote sensing can monitor water quality, and is a powerful support tool for assessing temporal and spatial variations in water quality of aquatic ecosystems, particularly in countries where water quality monitoring programmes are lacking (Concha and Scott, 2016).

To measure water surface temperature in lakes and reservoirs, remote sensing techniques have been commonly used (Ritchie, 2000). Several multispectral sensors with high resolutions such as Landsat, Sentinel, Moderate Resolution Imaging Spectroradiometer (MODIS), IKONOS, Medium Resolution Imaging Spectrometer (MERIS), Landsat TM and ETM+, Satellite pour l`observation de laTerre (SPOT), have been effectively used in large areas to estimate water quality variables of inland waters, including water surface temperature, water clarity, chl–*a* and total suspended solids (Ekercin, 2007; Blondeau–Patissier *et al*. 2014).

2.8 Multispectral sensors used in water quality monitoring

2.8.1 Landsat 7 Enhance Thematic Mapper Plus (ETM+)

Landsat series of satellites provides a data source for mapping and monitoring the surface. The Landsat sensors include the Landsat 7 which is equipped with ETM+ (Enhanced Thematic Mapper Plus) provides a ground survey in four modes: visible near infrared (VNIR), shortwave infrared (SWIR), panchromatic range, thermal infrared range. Landsat 7 ETM+ was launched on 15 April 1999 with a high spatial resolution of 30 m and visible through middle infrared channels and 120 m for thermal infrared band (Loveland and Dwyer, 2012). This has been widely used to estimate water quality parameters such as chlorophyll–a (Han and Jordan, 2005). Landsat 7 is still being operated in orbit for data collection, although the sensors have exceeded the expected service time and always readily experienced malfunction. The ETM + sensor has the same set of bands as the TM sensor but adds a 60 m thermal band and a 15 m panchromatic bands. To calibrate algorithms and minimise errors, nearly simultaneous ground observations are required when estimating water quality characteristics from Landsat data (Brezonik *et al.* 2005). The satellite carries the enhance thematic mapper.

Landsat 7 is good but the scan–line corrector (SLC) for the ETM+ sensor on board the satellite failed permanently on 31 May 2003. Efforts to recover the SLC was not successful, and this make the sensor line of sight trace to be a zig zag pattern along the satellite ground track. This also causes the image area to be duplicated with a width that increases towards the edge of the scene. When the Level–1 data are processed, the duplicated areas are removed, leaving data gaps (USGS and NASA, 2003). The SCL expressed the results in about 22 % pixels of the images that are unscanned. Therefore, the failure of the SLC (also known as the SLC–off problem) makes it difficult to use the Landsat 7 ETM+ data, while SCL also compensate for the forward motion. Under the abnormal circumstances, without an operating SLC on images, the wedge–shaped gaps that range from a single pixel in the width near nadir point for about 12 pixels found towards the edges of the scene (Pringle *et al*. 2009). Fortunately, the SLC–off has not been affected by the radiometric and geometric quality of the sensor. Approximately 80 % of the pixels in each image are being scanned (The USGS and National Aeronautics Space Administration [NASA], 2003).

2.8.2 Landsat 8 Operation Land Imager (OLI)

Landsat is the longest operating enterprise for satellite imagery acquisition of the earth (He *et al*. 2012; Dai *et al*. 2017). Among several satellite systems used to monitor water quality, the Landsat system offers a high coverage of the Earth's surface status and dynamics, is especially useful for the assessment of inland lakes and reservoirs (Kloiber *et al*. 2002b; Matthews, 2010; Chao Rodríguez *et al*., 2014). Landsat 8 operational land imager (OLI) was launched in 2013 with a high spatial and spectral resolution with the ability to detect and map water quality variables (Pahlevan *et al*. 2014; Franz *et al.* 2015).

The OLI has the enhancement capabilities of 30 m spatial resolution in the visible and near–infrared bands, and additional red–edge bands that allow the sensor to absorb very low chlorophyll–*a* concentrations. This has also allowed human impacts to be mapped from space such as quarrying (Barnes *et al*. 2015) and offshore construction to be resolved (Vanhellemont and Ruddick, 2014).

As a result of the high spatial resolution and atmospheric correction using shortwave–infrared bands, turbid rivers have been studied in more detail (Giardino *et al*. 2014; Ruddick *et al.* 2006), and various optically active constituents have also been retrieved. The key objective is to obtain features of surface temperature, heat and moisture transfer process in agriculture and water management (Concha and Schott, 2016). The water presents obstacles to monitoring systems for both in situ and remote sensing (Vanhellemont and Ruddick, 2016).

2.9 Previous studies on using remote sensing on monitoring water bodies

2.9.1 MODIS

The launch of Moderate Resolution Imaging Spectroradiometer (MODIS) was in 2002. The variation of spatial resolution of (2 bands at 250 m, 5 bands at 500 m and 29 bands at 1 km) MODIS comes with 36 spectral bands ranging in wavelength from 0.4 µm to 14.4 µm because of their spatial and temporal resolution are suitable for monitoring water turbidity (Lillesand, 2002). MODIS is a powerful imaging sensor, installed on two satellite platforms; Terra and Aqua launched in 1999 and 2002 respectively (Chen *et al*. 2015).

The orbits of Terra and Aqua satellites are designed revisit any location on the earth's surface approximately every 1 to 2 days, which means that temporal resolution of MODIS imagery is very suitable for spatiotemporal studies (Hou et al. 2017). Each MODIS image consists of 36 image bands that range from 400 to 14 400 nm wavelength and 250 to 1 000 m in spatial resolution. The Land Processes Distributed Active Archive Center (LP DAAC) is an agency that processes, archives, and distributes 68 different data items from MODIS data, such as surface reflectance, surface temperature and vegetation index (https://www.Ipdaac.usgs.gov; Doxaran *et al*. 2009).

Surface reflectance products are useful in extremely turbid water bodies because water is a strong reflector of the sun's radiation (Petus *et al*. 2014). The MYD09GQ image of Band 1 has spatial resolution of 250 m with a temporal resolution of 1 day and a wavelength centred at 645 nm. The reflectance of wavelength is susceptible to mineral suspended matters and water turbidity (Bowers *et al*. 2007). The estimation of chl-*a* concentration in waters with spectral algorithm based on reflectance in the near-infrared (NIR) (Dall`Olmo *et al.*, 2005). Using the reflectance data collected in the field with spectrometers, Dall`Olmo and Gitelson (2005) demonstrated that NIR and Red models given by three band NIR-Red model to give an accurate estimation of chl-*a* concentration for inland water bodies with the wide range of bio-physical and optical characteristics. The model has shown that NIR-Red models works well with waveband location and width to match the waveband of MODIS.

2.9.2 IKONOS

The amount of solar radiation transmitted by surface water at different wavelength is measured by remote sensing satellite, while the optical properties of water in this procedure depend on the concentration and character of the water quality parameters (Bilge *et al.* 2003). The water quality is correlated to in situ measurements and measured by solar radiation. The IKONOS satellite was successfully launched in 1999 as the first commercially available high resolution satellite sensor determined by water quality monitoring studies (Thenkabail *et al*. 2003). The spectral range of multispectral IKONOS imagery with high spatial resolution makes the sensors ideal for monitoring water quality. By observing the ratio of blue to red light in the satellite results, IKONOS is a false colour satellite that shows the water clarity and consistency of the reservoir (Arango and Nairn, 2019), by observing the blue to red light ratio in the satellite results. This indicates that the reservoir has high water quality because the amount of blue light reflected off the reservoir is high and red light is low. Therefore, algae and sediment loaded reservoirs show less blue light and more red light (Ozesmi and Bauer, 2002). IKONOS can capture 0.82 panchromatic resolution of 3.2 m multispectral, near–infrared (NIR) at nadir. In order to determine the water quality of water sources, a higher resolution satellite is needed. IKONOS's capabilities include recording a 0.82 panchromatic resolution of 3.2 m multispectral, near–infrared (NIR) at nadir. Four multispectral bands of IKONOS imagery are comparable to Landsat/TM bands 1–4 and high (4 m multispectral bands to 1 m panchromatic) spatial resolution by compiling the imagery to be a good candidate for applying previous methods to assess smaller lakes and reservoirs (LI., 2004). The algorithm to determine chl-*a* concentration in inland water were developed through simple linear regression analysis. Surface reflectance of each band and chl-*a* concentration values at a specific sampling point were regressed. The reflectance of all bands were selected to be independent for each value to form a relationship with reflectance by showing high coefficient of determination (R^2) (He *et al.*2008).

2.9.3 SPOT

Satellite pour l`observation de la terre (SPOT) images is characterised by three bands, near–infrared, red, and green light that are applied to detect water quality i.e., chl–*a* density, disk depth and total phosphorus density. The SPOT multifrequency images have a ground resolution of 20×20 m^2 and a panchromatic background resolution of 10×10m^2 (Yang *et al.,* 2000). To estimate phytoplankton growth and respiration rates, SPOT imagery is also applied to water quality monitoring of reservoirs. Usage of sensing data from SPOT and Landsat TM, in situ data and quality of water.

In the previous studies Semi imperial algorithm was deployed to estimate chl-*a* concentration in inland water bodies. These has shown a close relationship between chl-*a* concentration and Red-NIR ratios that estimate chl-*a* in reservoirs. Evidence shows that the 3D model could be employed to derive chl-a concentration in reservoir. the 3D modelrelates to chl-a pigments to reflectance in the spectral bands where λ_1 is in the red range (670nm) λ_2 should be in the range between 700-710 nm and λ_3 should be in the NIR between 700-750 nm (Gitelson and Dall`Olmo, 2006).

2.10 Spatial interpolation in water quality parameters analysis

The distribution of spatio–temporal of both physical and socio–economic occurrence can be estimated depending on the location of the multi–dimensional space, multivariate scalar, and vector fields (Neisi *et al*. 2018). Typical examples of multivariate fields are water, soil properties, population densities, and fluxes of organic matter, therefore most of these fields are characterised with measured data or digitised point data that are often distributed irregularly in space and time, visualization, modelling, and analysis based on raster representation in GIS. Moreover, various phenomena in the fields can be measured using remote sensing and site sampling (In–situ) leading to heterogenous datasets with a various digital representation and resolutions that need to be combined to create a single spatial model (Abbasnia *et al*. 2018).

The predicted values of spatial phenomena in unsampled locations were developed using with interpolation and approximation methods. The application of GIS in these methods were designed to support the transformation of different discrete and continuous representation of spatio–temporal fields for the transformation of different raster resolution. The modelled data are very complex in the application of GIS, while data are spatially heterogenous based on the optimal sampling and the significant noise that can be present (Lotfi, 2014). The dataset can be very large with different accuracies that have originated from different sources. The reliable interpolation tool should be able to satisfy different demands suitable for the applications of GIS. Spatial interpolation methods are frequently used to estimate values of the physical and chemical constituents in an area where they are not measured. Therefore, this can relatively investigate the performance of difference interpolation methods in the water environment (Belkhiri *et al*. 2014).

In recent years, with the increased number of physical and chemical water quality variables in the water environments and a broad scope geostatistical method are now utilized for a proper analysis and interpretation of information. Therefore, many researchers are concentrating more on the evaluation of spatial distribution of water quality using various statistical methods (Guettaf *et al*. 2014). Geostatistical methods are a helpful tool for analysing the structure of spatial variability, interpolating between point observations and creating the map of interpolated values with an associated error map. A few investigations have detailed that water quality is by and large described by a critical spatial variety. This proposes that geostatistical strategies, which are explicitly ready to join the spatial variability of water quality into the estimated processes the aught to be utilized. Nowadays, different geostatistical techniques methods are broadly used for the spatial variation of water quality (Nazari Zade *et al*. 2006). In GIS, there are three spatial interpolation methods (i) inverse distance weighting (IDW), (ii) ordinary kriging, and (iii) a universal kriging method that incorporate the output from the process–based water quality model that can be applied on surface water quality parameters such as temperature, salinity, chl–*a*, turbidity, pH, and total suspended solids to compare the analysis from different seasons (Zhou *et al*. 2014).

2.10.1 Kriging

Kriging is a stochastic technique like IDW and uses a linear combination of weights in the known locations to assess the data values of an unknown location. Variogram is an important input in kriging interpolation by measuring the spatial correlation between two points. Weights will vary depending on the spatial arrangement of the samples when using established variograms (Bekele *et al*. 2003). Kriging has the advantage of providing a measure of error or uncertainty of the estimated surface in addition to the estimated surface. The disadvantage requires a significantly and more processing time and user feedback when compared to IDW and spline (Longley *et al*. 2005).

Bekele (2003) compared IDW and kriging spatial interpolation discovered that kriging outperformed IDW in most cases, and came into conclusion that a regression–based autocorrelated error model was a more versatile form of interpolation in general. These is relatively more stable because is less dependent on the spatial structure. Kriging is one of geostatistical interpolation techniques that has a several number of variations, including simple kriging, ordinary kriging, co–kriging, stratified kriging, and non–linear kriging, with ordinary kriging used most frequently to map water quality variables and commonly applied in estimating spatial distribution of variables (Brus and Heuvelink, 2014).

2.10.2 Spline

Spline is a deterministic method that represents a two–dimensional curve on three–dimensional surfaces. This can be described as a mathematical function of fitting a flexible surface across a series of known points. Therefore, a major advantage of spline is being able to build reasonably consistent and visually pleasing surfaces with just a few sample points. The disadvantages are that the resultant surface that varies from the input data set in terms of minimum and maximum values are sensitive to outliers, and that there is no indication of errors (Longley *et al.* 2005).

Lasllet *et al*. (1987) found that, though each method could outperform the others in some circumstances, spline, and kriging outperformed IDW on average. Robinson and Metternicht (2006) have compared spline, kriging and IDW interpolation methods on water quality and found that, there was no approach that could be used in all cases. However, Simpson and Wu (2014) reported that when interpolating reservoir depth, comparison of IDW, kriging, and spline, was found that spline obtained the most accurate results with less than the ideal number of sampled points.

2.10.3 Inverse distance weighting (IDW)

Inverse distance weighting is one of the least complex and promptly accessible strategies in geo–statistical interpolation. Therefore, IDW depend on the assumptions of the value at an unsampled point that can be approximated as a weighted average of values at a point within a certain cut off distance (Shukla *et al*. 2020). This is because Inverse Distance Weighted interpolation (IDW) assumes that the closer the sample point is to the cell with the value is to be estimated, the more intently the cell's value will resemble the sample point's value (ESRI, 2005).

The principle underlying IDW is the Waldo Tobler's first law of geography which states that "everything is related to everything else, but near things are more related than distant things" IDW uses linear combination of weights at known points to estimate unknown location values. The IDW is easier than Kriging, yet a few investigations showed that this outperformed the last mentioned, therefore, IDW can also handle parameters that are not normally distributed (Hodam *et al*. 2017). The advantage of IDW is intuitive and effective and this works best with uniformly distributed points and is sensitive to outliers. While the disadvantage of IDW is sensitive to outliners and that they are no indications of error. The unevenly distributed data brings out the results of introduced errors (Sapna *et al*. 2018). According to Schloeder *et al*. (2001), the IDW, kriging, and spline spatial interpolation methods has concluded that IDW and kriging performed similarly, and both are more precise than spline interpolation method.

2.11 Land use and land cover implication on water quality using remote sensing

Land use land cover (LULC) are two separate terms that are used interchangeably. Land cover is defined as a physical feature of earth`s surface including vegetation, water, soil, and other physical features created by human activities such as settlements, while land use refers to land used by human beings for residential and economic activities (Rawat and Kumar, 2015). Land use land cover pattern depend on human usage related to natural and socioeconomic development over space and time. Shifting into possibility of negative impact of Land Use for social activities affecting land cover changes, especially in relation to biodiversity and water (Khan *et al*. 2015; Olusola *et al.* 2018).

These changes are applied to only one main factor in terms of size and pattern, namely, population growth. Population growth contributes directly and indirectly to changes in LULC, especially from the point of view of demand for built-up area in agricultural activities, and water resources. Ecological experts are interested in how LULC changes affect biodiversity and aquatic ecosystems. Changes in land cover in the watershed will affect water quality, resulting to increased surface runoff, reduced groundwater discharge, and transfer of pollutants (Butt *et al.* 2015). Therefore, land use land cover information at the watershed level is important for the selection, planning, monitoring, and management of water resource so that changes in land use respond to the increasing demand of human needs and welfare without compromising water quality. Land use land cover changes in the watershed area due to urbanization and deforestation will continuously have a negative impact on water quality and indirectly affect the nature of the watershed ecosystem. Therefore, understanding of the spatial and temporal variations occurring in the watershed over time as well as explaining the interactions between hydrological components of the watershed which enable the development of good water conservation strategies (Matshakeni, 2016; Nabeela *et al.* 2014).

Remote sensing has been widely used to classify and map LULC changes with different techniques and data sets, such as Landsat images that provide better classification of different landscape components at a large scale (Hansen and Loveland 2012). Several changes of detection techniques have been developed in remote sensing images with debate over advantages and disadvantages of each technique. These includes unsupervised classification or clustering, supervised classification techniques applied on LULC changes. Various classification techniques have been proposed, and supervised classification methods were considered as favorable for change detection analysis. In recent studies, researchers have applied supervised classification for several LULC change (Mahmud and Achide, 2012).

CHAPTER THREE: MATERIALS AND METHODS

3.1 Study area

Nandoni reservoir (22°59'20"S 30°36'27"E) is located on the Luvuvhu River approximately 16 km southeast of Thohoyandou, Limpopo Province, South Africa (Fig. 1). The surface area of the reservoir is 1 650 ha and is located in a humid and hot region with summer rainfall. The mean annual rainfall in the catchment is 800 mm. The general absence of buffer vegetation along inlets, streams, and the reservoir intensify the threats to Nandoni reservoir's water quality (Dalu *et al*. 2019). The reservoir was established by the Department of water and Affairs and Forestry in 2005 to upgrade the former Mutoti reservoir. The reservoir was completed in 2009 and the water carrying capacity is estimated at 164 million m^3 (DWARF, 2004b) and catchment area is 1380 km^2.

The reservoir was designed to supply water to 1.3 million people in the Vhembe and Mopani Districts. Nandoni reservoir releases water downstream to supply water for wildlife in the Kruger National Park. Along the shorelines of Nandoni reservoir, there are four villages with poor service delivery and extreme poverty. The reservoir is extremely important to the surrounding communities in terms of ecology, culture, and economics. Three zones where randomly selected across the reservoir: river zone (sites 23–26), middle zone (sites 11–22) and dam zone (sites 1–10). Survey was conducted over hot–wet season (December 2020).

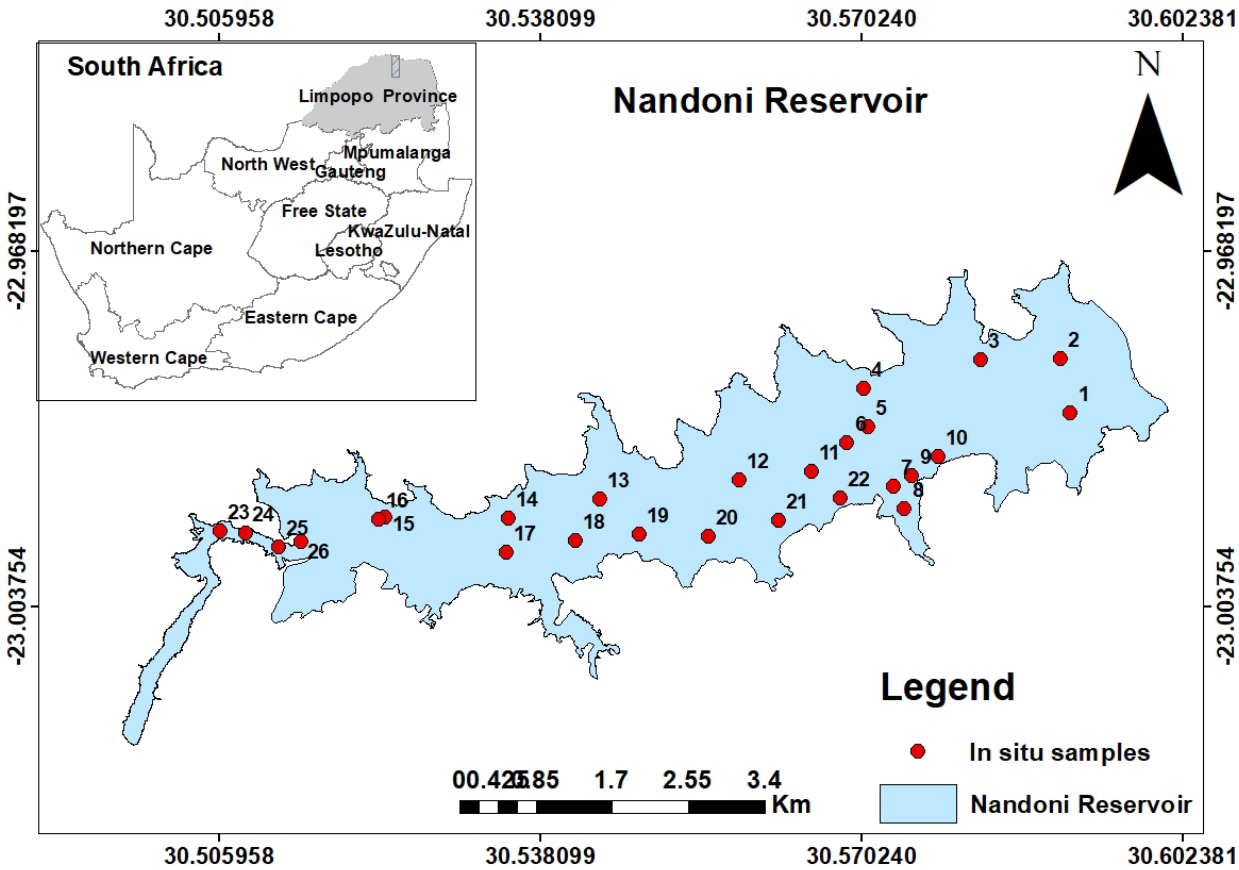

Fig. 1. The map showing the location of the study sites in Nandoni Reservoir, South Africa

Samples were collected from the 3rd to 5th of December 2020 under clear skies between 9:00 am and 12 PM, so that diurnal changes and water quality can be controlled. The collection of water samples on the first sampling day were conducted for sites 1–10, second day water samples were collected from sites 11–22, and the third sampling day for sites 23–26.

3.2 In–situ physico–chemical measurement and water collection for chlorophyll–*a* concentration

A boat was used to collect water samples for chlorophyll–a concentration determination and for in–situ measurement of physico–chemical parameters along the reservoir entire length across the 26 randomly selected sites. Temperature (°C), pH, electrical conductivity (µS/cm), total dissolved solids (TDS; ppm), resistance (Ω), oxidation–reduction potential (mV) and salinity (ppm) were measured in situ at all sites using portable handheld PCTestr 35 multi–parameter probe (Eutech / Oakton Instruments).

Water samples for chlorophyll–*a* concentration analysis were collected using 1 litre Consol glass bottles. Integrated water samples (n = 2 per site) from the aquatic ecosystem were taken below the surface, by directly holding the bottle into the water at a depth of 30 cm below the surface. Extreme care with the water sample bottles were taken to ensure that no air bubble was left inside. All bottles were marked with the site number after the collection. The samples were stored in a cooler box on ice before being taken to the laboratory for further analysis.

3.3 Chlorophyll–*a* concentration analysis

The chl–*a* concentration can also be used to estimate phytoplankton biomass in aquatic ecosystems (Shen *et al*. 2008). Chlorophyll–*a* measurements in the laboratory were done to give a proxy of the phytoplankton biomass present in the water. In the laboratory, 250 mL of sampled water were filtered through 0.07 µm glass fibre filter (GF/F). Each filter paper was folded into quarters and wrapped in aluminium foil and place them in the dark, to protect the extracts from the light. To these, 10 mL of 90 % acetone was added to each filter paper removed from aluminium foil in centrifuge tubes to determine the total chl–*a* concentration as described in Dalu *et al*. (2013b) and incubated immediately for 24 hours at –20 °C in the freezer to wait for the analysis in the laboratory. After 24 hours, the extract was filtered to remove any materials in suspension. Chlorophyll–*a* concentration were determined by using spectrophotometry method which involves the use of spectrophotometer analysis, where the absorbance of the processed samples was recorded at selected wavelengths of 665 nm and 750 nm following the protocol of Strickland and Parsons (1960) for calculating chl–*a* concentration (Almomani *et al.* 2018). The 1 mL of chl–*a* samples were filled in a disposable semi–micro cuvette for the analysis of chl–*a* fluorescence in a SPECTROstar NANO (BMG Labtech GmbH, Ortenberg) to measure the spectrum absorbance of chl–*a* concentration in the water samples using the same selected wavelength of 665 nm and 750 nm to determine before and after of chl–*a* concentration in all water samples.

3.4 Physico–chemical parameters trend analysis using GIS

In this project, geo–statistical analysis was used to analyse water quality parameters in ArcGIS being employed to generate surface prediction maps for different values of the water quality parameters. The geostatistical analysis tool allows for the selection of different kriging methods, however in this project ordinary kriging was used. Ordinary kriging method was used to monitor the reservoir water quality. Therefore, this recommends the most reasonable focuses for finding the observing stations along the reservoir, considering the Kriging estimation errors (estimation variances) for the parts of the water quality variables (Murphy *et al.* 2010). The different values of the water quality parameters sum up to a unity, and by using a subset of neighbouring points to produce an interpolation.

3.5 Remote sensing Imagery Acquisition and pre–processing

Landsat–7 Enhanced Thematic Mapper Plus (ETM +) and 8 Operational Land Imager (OLI) datasets were used in this study. Images from 2008-2019 were acquired to compare the spatial distribution of chl-*a* with the year 2020 over Nandoni Reservoir.

3.5.1 Landsat 7 ETM+

Landsat 7 ETM+ has the potential to estimate water quality variables in water ecosystems (Torbick, 2008). Six medium spatial resolution (30 m) images were acquired from Landsat ETM+ over Nandoni Reservoir for the year 2008–2012 (see Table 1 for acquisition dates) to derive chlorophyll–*a* from the selected sites. Images were acquired under clear sky condition.

In addition, Landsat ETM+ includes seven multi–spectral bands with 30 m spatial resolution for all bands except band 6 with a thermal infrared band (TIR) of 60 spatial resolution and 15 m panchromatic band which covers 0.52–0.90 µm. All acquired images for different years for scenes: row 074 and path 169 were freely obtained from the United State Geological Survey (https://earthexplorer.usgs.gov). Images with cloud cover of approximately 75 % were excluded over the reservoir to ensure the accurate retrieval of chlorophyll–*a* concentration (Ndungu *et al*. 2013). Images acquired from ETM+ were atmospherically corrected. All images acquired from Landsat ETM+ were used to represent chl–*a* distribution within the reservoir.

3.5.2 Landsat 8 OLI

Eight cloud free images were downloaded for wet and dry season and were used for analysis in the current study. The image characteristics include the acquisition time, cloud coverage, path/row, and spatial resolution (Table 1). All standard Landsat 8 surface reflectance products were acquired from USGS Earth Explorer data portal (https://earthexplorer.usgs.gov). Data was retrieved at 30 m spatial resolution through using Landsat surface reflectance where the satellite overpasses the reservoir. Landsat OLI data were acquired as a source to estimate chl–*a* concentration within Nandoni reservoir. Eight images for hot–dry and cool–dry season were used to detect chl–*a* which covers Nandoni reservoir. These images were chosen based on the availability of data on in situ water quality, and cloud–free conditions. The parameter used in this study was chl–*a* that was obtained from the reflectance data of Landsat 8 OLI images. The acquired images were used to represent the distribution of chl–*a* variables. Images provided by the USGS for Landsat OLI were in digital number format (DN) for chl–*a* to be derived to calibrate the acquired images of top–of–atmosphere spectral radiance units that were based on the algorithm (Finn *et al*. 2012).

Table 1: Landsat specification of the satellite data used in the current study

Sensor	Band names	Ground sampling distance (km)	Acquisition date	Spectral resolution	Atmospheric condition
Landsat 7 ETM+	Red, blue, green, NIR, SWIR1,Thermal,SWIR2, Panchromatic	15	2008–07–27	30m	Clear condition
Landsat 7 ETM+	Red, blue, green NIR, SWIR1,Thermal,SWIR2, Panchromatic	15	2008–08–28	30m	Clear condition
Landsat 7 ETM+	Blue, green, Red, NIR, SWIR1,Thermal,SWIR2, Panchromatic	15	2010–08–08	30m	Clear condition
Landsat 7 ETM+	Blue, Green, Red, NIR, SWIR1,Thermal,SWIR2, Panchromatic	15	2010–12–24	30m	Clear condition
Landsat 7 ETM+	Blue, Green, Red, NIR, SWIR1,Thermal,SWIR2, Panchromatic	15	2012–05–19	30m	Clear condition
Landsat 7 ETM+	Blue, green, Red, NIR, SWIR1,Thermal,SWIR2, Panchromatic	15	2012–09–24	30m	Clear condition
Landsat 8 OLI	Coastal, Blue, Green, Red, NIR, SWIR 1, SWIR 2, Pan	30	2014–06–18	30m	Clear condition
Landsat 8 OLI	Coastal, Blue, Green, Red, NIR, SWIR 1, SWIR 2, Pan	30	2014–11–09	30m	Clear condition
Landsat 8 OLI	Coastal, Blue, Green, Red, NIR, SWIR 1, SWIR 2, Pan	30	2016–07–09	30m	Clear condition
Landsat 8 OLI	Coastal, Blue, Green, Red, NIR, SWIR 1, SWIR 2, Pan	30	2016–11–30	30m	Clear condition

Landsat 8 OLI	Coastal, Blue, Green, Red, NIR, SWIR 1, SWIR 2, Pan	30	2018–05–12	30m	Clear condition
Landsat 8 OLI	Coastal, Blue, Green, Red, NIR, SWIR 1, SWIR 2, Pan	30	2018–11–04	30m	Clear condition
Landsat 8 OLI	Coastal, Blue, Green, Red, NIR, SWIR 1, SWIR 2, Pan	30	2020–06–02	30m	Clear condition
Landsat 8 OLI	Coastal, Blue, Green, Red, NIR, SWIR 1, SWIR 2, Pan	30	2020–12–11	30m	Clear condition

3.6 Estimation of chlorophyll–*a* concentration from Landsat data

The processing of Landsat 8 OLI and 7 ETM+ was done using ENVI 5.1 and ARCGIS 10.7 software for cropping and algorithm input of images. Cropping was used to reduce image coverage in accordance with the study area. The algorithm was used on the coefficient provided with the dataset in a GIS environment to convert the reflectance value of images into chl–*a* concentration values based on ITTVIS (2009). Landsat 7 ETM+ and 8 OLI visible (VIS) and near infrared (NIR) spectral bands were used to retrieve chl–*a* over Nandoni reservoir. The ENVI 5.1 software was used to process radiometric correction and calibration, cropping and algorithm input on the chl–*a* raster image. To convert image pixels into reflectance values, radiometric calibration was used. Sun angle corrections are performed to correct error reflectance values caused by sun positioning. However, surface reflectance data were obtained by applying atmospheric correction with fast line-of-sight atmospheric analysis of hypercubes (FLAASH) algorithm (ENVI, 2009).

The ArcGIS 10.7 was used to perform the data image validation and classification after the raster data was created (Roy *et al*. 2014). The data processing using ArcGIS software was used to produce the distribution of chl–*a* map. All ETM+ images acquired for this study, from 2008 to 2012 with Scan Line Corrector (SLC) due to instrument problems and resulted to stripping (no data) across the imagery were de–stripped using QGIS 3.16 version software as a corrector tool (Wang *et al*. 2006). All images were corrected and calibrated and later converted according to chl–*a* concentration values. The reason to used gap–filling or de–stripping on Landsat ETM+ archives was to analyse the trend of chl–*a* in the reservoir. The spectral bands at 663 and 885 nm were used for extracting chl–*a* concentration from remotely observed reflectance measurements since this is where chl–*a* absorption was maximum.

3.7 Land use and land cover analysis using GIS

Supervised and unsupervised classification methods were adopted. Therefore, unsupervised classification algorithm was used to have an idea on land use and land cover cluster pixels. Supervised classification was used with the maximum classification approach. These algorithms they consider spectral variation within each category and covering different classes of land use and land cover (Rawat *et al*. 2015).

Land use land cover classified files used, were downloaded from the Department of Environmental Affairs (http://egis.environment.gov.za/gis_data_downloads), and then imported to ArcGIS 10.7 where composite maps were produced and show land use and land cover of Nandoni reservoir. Student t–test of Land use and Land cover was carried out using EXLSTAT to test hypothesis from normally distributed population.

3.8 Data analysis

3.8.1 Physiochemical variables

The assessment of water physico–chemical composition was based on the set of data consisting of 7 water quality variables measured in Nandoni reservoir. The analysis of the physico–

chemical variables among sampling sites and zones was carried out using One–way ANOVA to determine the significance results of physico–chemical variable in reservoir zones, using SPSS 21.0 software (SPSS Inc. 2017). Prior to data analysis, a non–parametric test, Kruskal–Wallis test was conducted to test the spatial distribution of in–situ chl–a concentration between sampling zones.

Pearson correlation was conducted to test the relationship that existed between chl–a and physico–chemical variables. The unsupervised analysis of in situ chl–*a* concentration was conducted to test similarities and dissimilarities of the chl–*a* concentration among sampling sites using cluster analysis with the Euclidean distance as a measure to determine spatial trends of the variables across the reservoir. Sampling sites with similar characteristics were grouped together to form homogeneous clusters (Kazi *et al*. 2009).

3.8.3 Remote sensing data analysis of chlorophyll–*a* concentration

In estimating chl–*a* concentration from reflectance value, spectral bands 445 and 665nm are very crucial, because that is where chl–*a* absorption is at peak, while the lowest chl–*a* absorption is found at 520 and 550nm (Dube, 2012; Dube *et al*. 2014). Based on this knowledge, this study employed the most popular chlorophyll–*a* estimation method (Buditama *et al*. 2017) to derive chl–*a* estimates over Nandoni reservoir from Landsat 7 ETM+ and Landsat 8 OLI images.

The following equation was used to extract chlorophyll–*a* concentration from both satellite images.

*Log Chl–a = (2.41*NIR/RED) + 0.187………………………………………………Equation 1*

*Log Chl–a = (2.41*NIR/RED) + 0.187*..*Equation2*

Where log = logarithm, chl-*a* = chlorophyll-*a, B4=RED, B5=NIR and B3=RED, B4=NIR*

After employing the above algorithm an output was created on ArcGIS with Logarithm spectral reflectance values. However, an anti- logarithm has to be introduced in order to remove the logarithm on the processed images to derive accurate chl-*a* concentration values instead of Logarithmic chl-*a* estimate

The following equation was used to calculate chlorophyll–a concentration in water samples.

Chlorophyll–$a = \frac{11.4 \times 2{,}43(E665 - EE750) - (E665 - E750) \times Vacetone}{L \times Vf}$ ....*Equation 3*

Where $Ewavelength$ = absorbance at wavelength, $Vacetone$ = volume of acetone used for extraction (mL), V_f = volume of water filtered (L), and L =path length of the spectrophotometer (cm), Concentrations are in unit µg/L.

3.8.4 Evaluation of remotely sensed derived chl–*a* estimates

Chlorophyll–*a* field measured data was transformed using the $\log_{10}$ (x+1) to meet the assumptions of normality and homogenous. Distance based Permutational Analysis of Variance (PERMANOVA) was conducted using PRIMER v6 add on package analyse spatial and temporal variation of chl–*a* concentration among the years, months, and zones on Euclidean distance. PERMANOVA uses permutation methods to assess the simultaneous response of several variables to several factors. Each term was using 9999 random permutations. The average dissimilarities of chl–*a* concentrations were checked for homogeneity using the permutation test of multivariate dispersion. (Bowling *et al*. 2016).

Landsat images that have be derived for chl–*a* concentration was validated using field chl–*a* measurements. The validation was carried out to determine the accuracy of remotely sensed chl–a estimates. The relationship between in situ and Landsat imagery were validated by counting the Root Mean Square Error (RMSE) between specified sampled data of the image processing with in–situ measurement obtained from the field survey. The RMSE uses the equation below:

$$\text{RMSE}=\frac{\sqrt{\sum(\text{Zi}-\text{Z}j)}}{n} \quad \ldots\ldots\ldots\ldots\ldots\ldots\ldots\ldots\ldots\ldots \textit{Equation 4}$$

Where *Zi* is Landsat imagery data, *Zj* is the measured chl–*a* in situ data and *n* is the number of sampling sites.

CHAPTER 4: RESULTS

4.1 Physico–chemical variables

The distribution of physico–chemical variables measured in Nandoni reservoir during the ground–truthing in December 2020 is highlighted in Figure 2. In the river zone, conductivity ranged between 273 and 276.7 µS cm^{-1} (mean 8.09 ± 0.34 µS cm^{-1}), with levels increasing towards the middle zone. In the middle zone, conductivity decreased towards the dam zone. The mean conductivity values in the middle and dam zones were 8.65 ± 0.06 µS cm^{-1} and 8.62 ± 0.22 µS cm^{-1} (Figure 2a; Table 2). The oxygen reduction potential (ORP) was high in a small bay in the dam zone, with values in this zone ranging from –96.2 to –101.4 mV. In general, the ORP values were relatively low in the river zone, with mean of –71.5 mV (range –59.6 to –77.8 mV; Figure 2b, Table 2). The salinity was generally high in the river zones (mean 274.9 ± 1.29 ppm) towards the centre of the middle zone, before declining towards the dam zone (mean 124.6 ± 3.37 ppm; range 118.0 – 129.3 ppm; Figure 2c). The total dissolved solids (TDS) were relatively high from the river zone with values ranging from 137.2 to 141.2 mg L^{-1} (mean 139.7 ± 1.4 mg L^{-1}) and decrease towards the small bay in the dam zone with values ranging from 41.0 to 50.6 mg L^{-1} (mean 43.8 ± 2.4 mg L^{-1}; Figure 2d). The pH was relatively high in middle zone with values ranging from 8.4 to 8.7 (mean 8.7 ± 0.06) and decline in the river zone with values ranging from 7.3 to 9.3 (mean 8.1 ± 0.34) and dam zone (mean 8.62 ± 0.2; Figure 2e, Table 2). Temperature was high in the middle zone with values ranging from 26.5 to 27.9 °C (mean 27.1± 0.39 °C). The temperature values in the dam and river zone declined with values ranging from 26.7 to 27.9 °C (mean 27.19 ± 0.4 °C) and 24.8 to 25.7 °C (mean 25.2 ± 0.29 °C; Figure 2f). Resistivity was relatively high in a small bay in the dam zone with values ranging from 3.0 to 3.4 Ω (3.3 ± 0.1 Ω) and in the river zone ranging from 3.5 to 3.1 Ω (mean

3.6 ± 0.02 Ω). In general, resistivity values declined in the middle zone with (mean 3.3 ± 0.1; Figure 2g, Table 2).

Table 2. Mean (± standard deviation) and range of physico–chemical variables in Nandoni reservoir for the different zones. Abbreviations: ORP – oxygen reduction potential, TDS – total dissolved solids

Variable	**Units**	**Dam Zone**		**Middle Zone**		**River Zone**	
		Mean ± SE	**Range**	**Mean ± SE**	**Range**	**Mean ± SE**	**Range**
pH		8.62 ± 0.2	7.9 – 8.9	8.7 ± 0.06	8.4 – 8.7	8.1 ± 0.34	7.3 – 9.3
Temperature	°C	27.19 ± 0.4	26.7 – 27.9	27.1 ± 0.39	26.5 – 27.9	25.2 ± 0.29	24.8 – 25.7
Salinity	ppm	124.6 ± 3.4	118.0 – 129.3	133.6 ± 0.9	131.4 – 134.5	134.1 ± 0.8	133.0 – 135.0
Conductivity	$\mu S\ cm^{-1}$	273.4 ± 57.7	28.5 – 292.4	268.1 ± 26.3	144.8 – 276.1	274.9 ± 1.3	273.0 – 276.7
TDS	$mg\ L^{-1}$	43.8 ± 2.4	41.0 – 50.6	149.5 ± 2.5	144.2 – 153.1	139.7 ± 1.4	137.2 – 141.2
Resistivity	Ω	3.3 ± 0.1	3.3 – 3.4	3.3 ± 0.1	3.3 – 3.4	3.6 ± 0.02	3.5 – 3 .1
ORP	mV	–99.5 ± 1.4	–101.4 to –96.2	–99.4 ± 1.4	–101.4 to –96.2	–71.5 ± 7.1	–77.8 to –59.6

Using a one–way ANOVA analysis, significant differences were observed for salinity ($F = 104.60$, $p < 0.001$), TDS ($F = 1.22$, $p < 0.001$), resistivity ($F = 90.44$, $p < 0.001$), and ORP ($F = 296.47$, $p < 0.001$) among the different reservoir zones, whereas conductivity ($F = 0.132$, $p = 0.877$) was found to be non–significant. Based on Tukey's post hoc analysis, non–significant differences ($p > 0.05$) were observed on dam *vs* middle zones for pH, temperature, and resistivity, and middle *vs* river zones for salinity, and for all zones for conductivity.

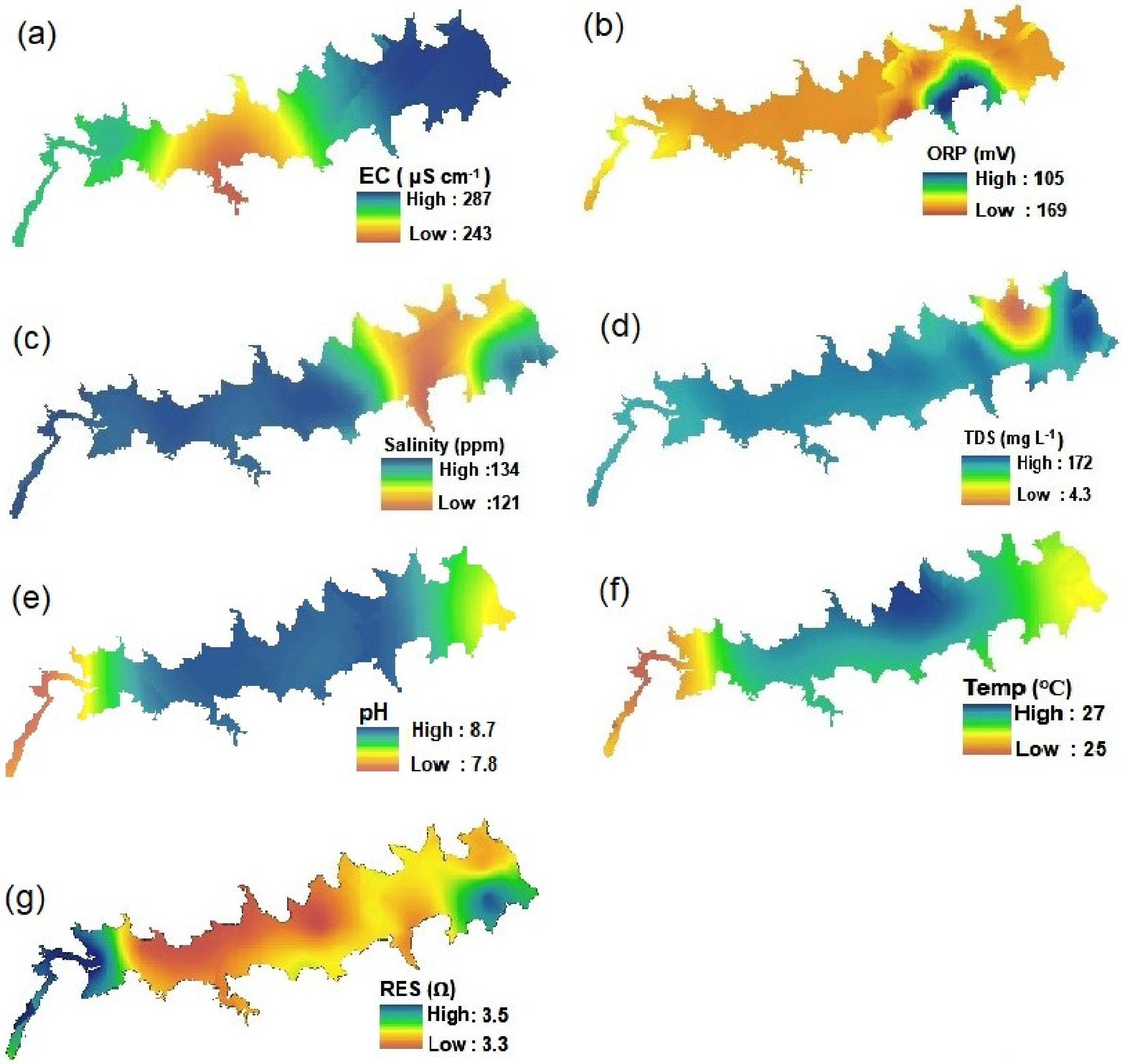

Figure 2. The distribution of physio–chemical parameters: (a) conductivity, (b) oxygen reduction potential (ORP), (c) salinity, (d) total dissolved solids (TDS), (e) pH, (f) temperature (temp) and (g) resistivity (res) measured in–situ in December 2020 in Nandoni reservoir

4.2 Land use and land cover variation around Nandoni reservoir environs

In this study, settlement, agriculture, open and closed savanna, and bare ground were revealed as the main land use and land cover type around the Nandoni reservoir. The reservoir intermediate catchment area is dominantly occupied by open savanna (37.8 %), with settlements constituting 36.0 % of the land use and land cover type (Figure 3). Agriculture occupies (14.1 %) and close savanna (10.0 %) and bare ground (1.5 %) occupies smallest portion of the catchment (Figure 3). Student t–statistic has highlighted a non–significant difference ($t = 2.606$, $p > 0.05$) among the land use and land cover types.

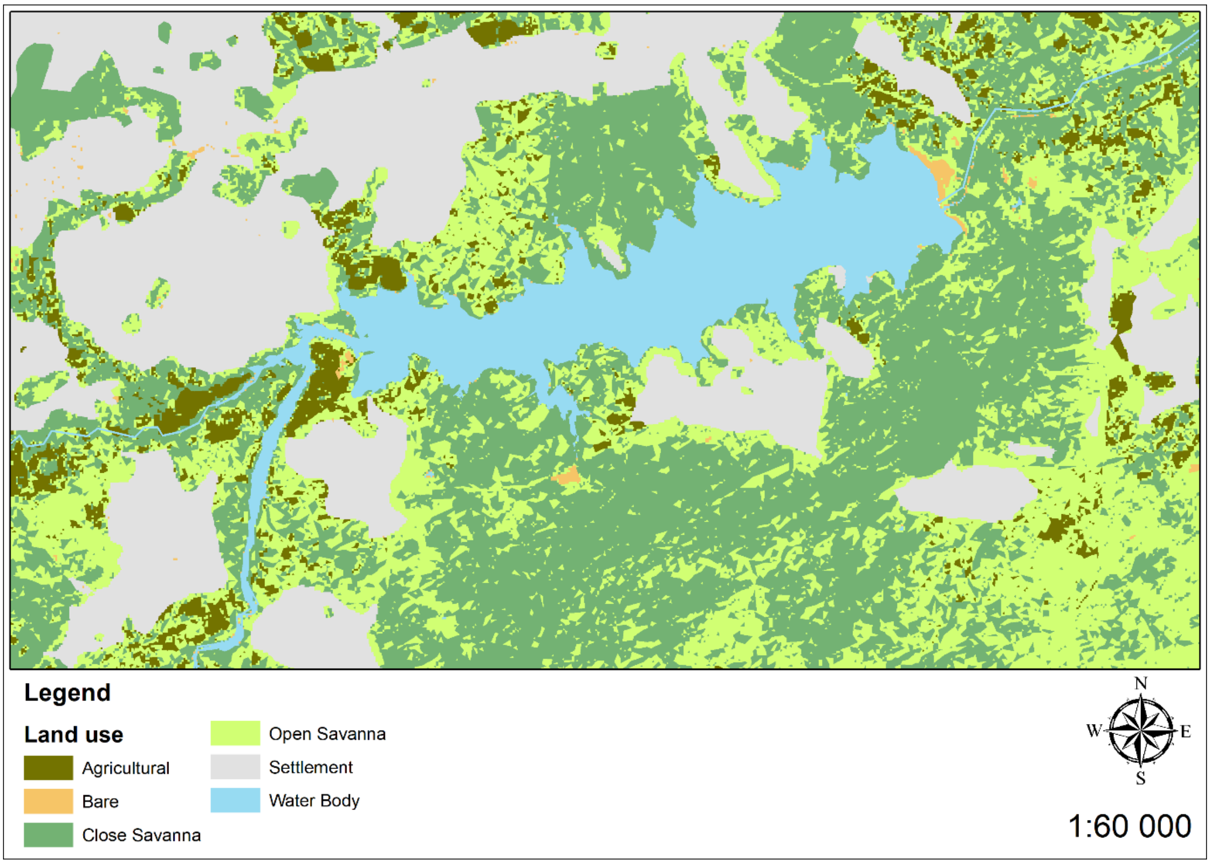

Figure 3. Land use and land cover variation of Nandoni reservoir.

4.3 Chlorophyll–*a* concentration maps

4.3.1 Field measured chlorophyll–*a* concentration

The distribution of chl–*a* concentration measured in Nandoni reservoir in December 2020 is highlighted in Figure 4. In the dam zone, chl–*a* concentration was high near the dam wall and in a small bay with values ranging from 0.3 to 1.46 $\mu g\ L^{-1}$ and decreased towards the middle zone with concentrations ranging from 0.2 to 0.8 $\mu g\ L^{-1}$. Chlorophyll–*a* concentration was low in the river zone with values ranging from 0.2 to 0.6 µg L^{-1} and also sections of the middle zone. Kruskal–Wallis highlighted significant differences (H = 2.978, d*f* = 2, *p* = 0.014) among the reservoir zones.

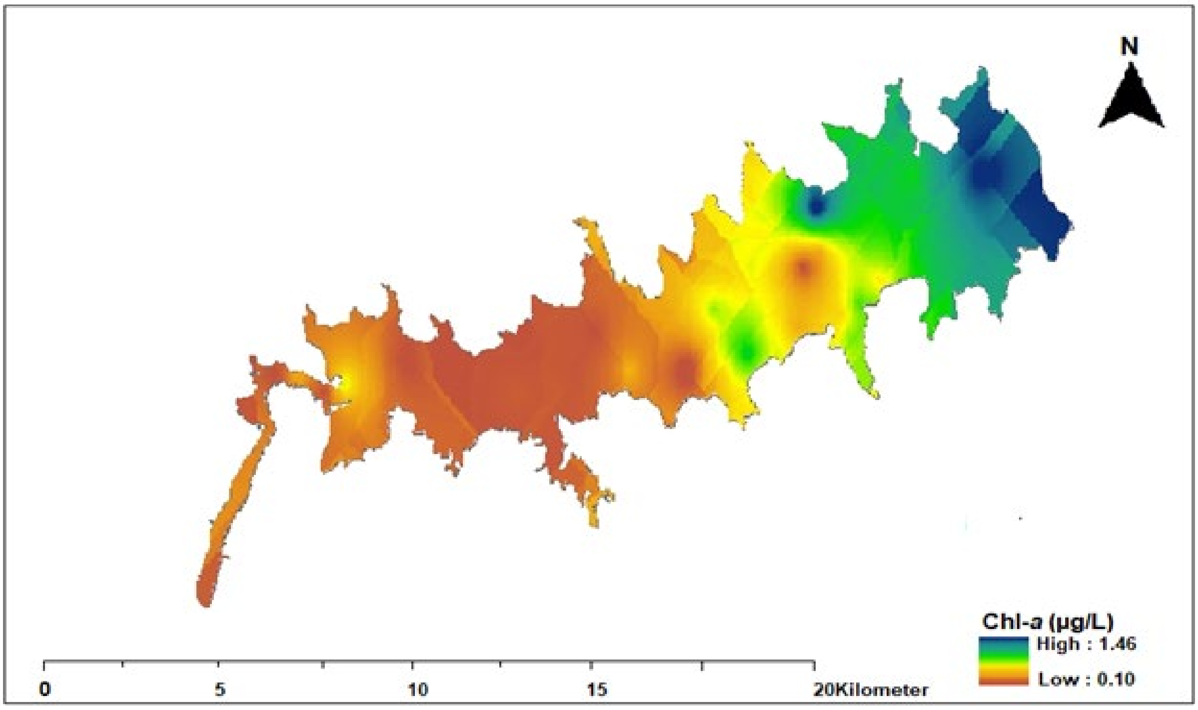

Figure 4. Spatial distribution of in–situ measured chlorophyll–*a* concentrations from Nandoni reservoir, South Africa.

4.3.2 Relationship between chlorophyll-*a* concentration and physico-chemical variables.

Cluster analysis (CA) grouped chl–*a* concentration from 26 sites sampled in December 2020 into four clusters. *Cluster 1* had site 6, *cluster 2* had four sites (sites 23 – 26), *cluster 3* had 12 sites (sites 11 – 22), and *cluster 4* included 9 sites (7 – 10, 1 – 5) (Figure 5). *Clusters 1* and *4* consisted of the dam zone sites, *cluster 2* consisted of river zone sites and cluster 3 consisted of sites from the middle zone of the reservoir.

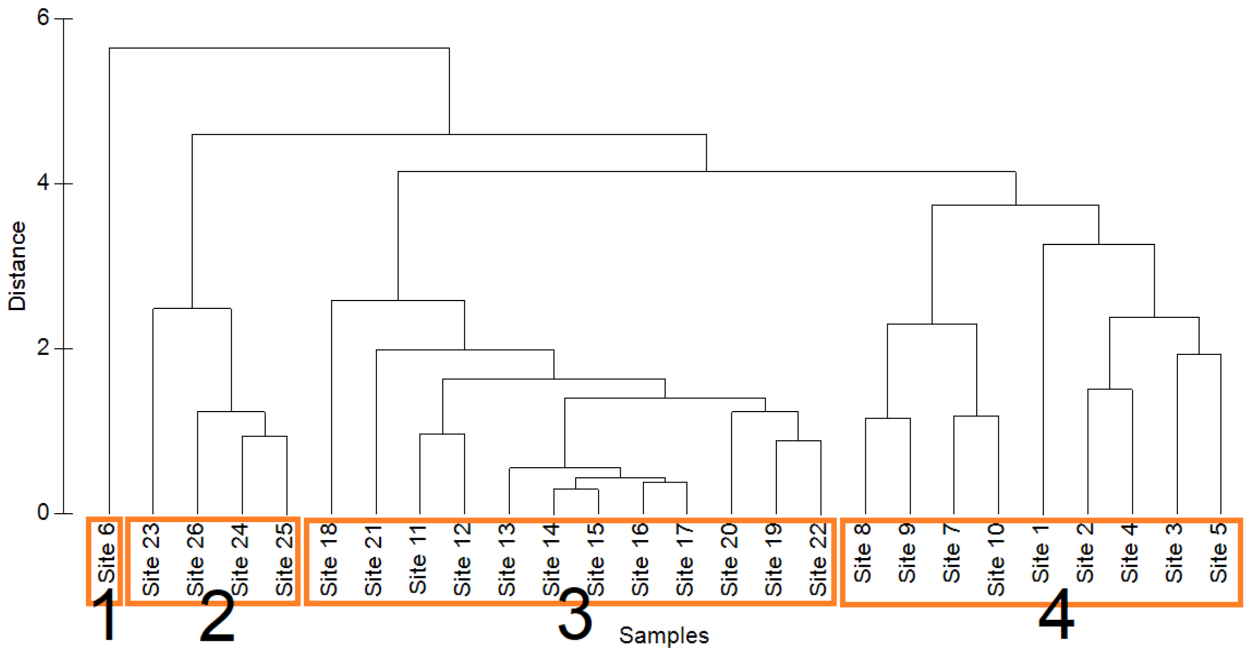

Figure 5. Cluster analysis results for the chlorophyll–*a* concentration for the field recorded values in Nandoni reservoir, South Africa

The relationship that existed between chl–*a* concentration and physico–chemical variables was assessed using the Pearson correlation, with non–significant negative (resistivity: $r^2 = -0.17$, $p = 0.242$; ORP: $r^2 = -0.14$, $p = 0.321$) and positive (pH: $r^2 = 0.01$, $p = 0.941$; conductivity: $r^2 = 0.17$, $p = 0.222$) relationships being observed for selected physico–chemical and chl–*a* concentrations. Significant positive relationships were observed for water temperature ($r^2 = -0.28$, $p = 0.048$) with chl–*a* concentration, with strong significant negative relationships being observed for salinity ($r^2 = -0.41$, $p = 0.003$) and TDS ($r^2 = -0.44$, $p = 0.001$) with chl–*a* concentration.

4.3.3 Remotely sensed chlorophyll–*a* concentration values across seasons and years

During dry season in the year 2008, chl–*a* concentration values ranged from 7.0 – 0.5 µg L^{-1} in the river zone and low towards the middle and dam zone (Figure 6). In 2010, chl–*a* concentration was high in the river zone with values ranging from 3.8 – 1.3 µg L^{-1} (Figure 6).

In the year 2012, chl–*a* concentration was high in the river zone with values ranging from 3.5 to 0.9 µg L^{-1} and low in the middle and dam zone (Figure 6). In 2014, concentration values were high in the shorelines and river zone ranging from 4.4 – 2.1 µg L^{-1} and low towards the middle zone and dam zone (Figure 6). In 2016, the reservoir was at low capacity during the prevailing drought conditions and chl–*a* concentration declined towards the middle and dam zones with values ranging from 4.8 – 2.0 µg L^{-1} (Figure 6). Concentration values in the year 2018 was high in a small bay in the river zone with values ranging from 5.9 – 2.1 µg L^{-1} in and concentration declined towards the middle and dam zone (Figure 6). In 2020 the concentration values were ranging from 5.1 – 2.2 µg L^{-1} in the river zone and low in the middle and dam zone (Figure 6).

During the wet season in year 2008, chl–*a* concentration in the reservoir were high ranging from 7.0 – 0.5 µg L^{-1} in the river zone and low in the middle zone moving towards the dam zone (Figure 6). In year 2010, chl–*a* concentration values were high in a small bay in the river zone of the reservoir with values ranging from 5.0 to 0.9 µg L^{-1} and low in the middle zone towards the dam zone (Figure 6). In year 2012, chl–*a* concentration ranged from 4.6 to 0.8 µg L^{-1} in the river zone and low concentrations were recorded in the middle zone and dam zone (Figure 6). In the year 2014, chl–*a* concentration was high in a small bay in the river zone and shorelines ranging from 2.3 to 5.3 µg L^{-1} (Figure 6). In year 2016, chl–*a* concentrations were low ranging from 2.1 to 4.7 µg L^{-1} in the river zone increasing towards the middle and dam zones (Figure 6). In year 2018, chl–*a* concentration values were detected in the river zone ranging from 2.3 to 6.0 µg L^{-1} and declined towards the middle zone, concentration also increased in the dam zone (Figure 6). In the year 2020, chl–*a* concentration values were high in a small bay in the river zone ranging from 2.2 to 7.0 µg L^{-1} and low concentrations were recorded in the middle and dam zones (Figure 6).

Chlorophyll–*a* concentration significantly varied between the years ($F_{6,364} = 10.57$, $p < 0.0001$), seasons ($F_{1,364} = 5.767$, $p = 0.0170$) and zones ($F_{2,364} = 6.843$, $p = 0.0010$). Furthermore, significant interaction variation was observed for seasons × year ($F_{6,364} = 94.096$, $p < 0.0001$), and year × zones ($F_{12,364} = 5.468$, $p < 0.0001$), with no significant differences being observed for seasons × zones ($F_{2,364} = 0.113$, $p = 0.8930$) and seasons × year × zones ($F_{12,364} = 1.118$, $p = 0.3450$).

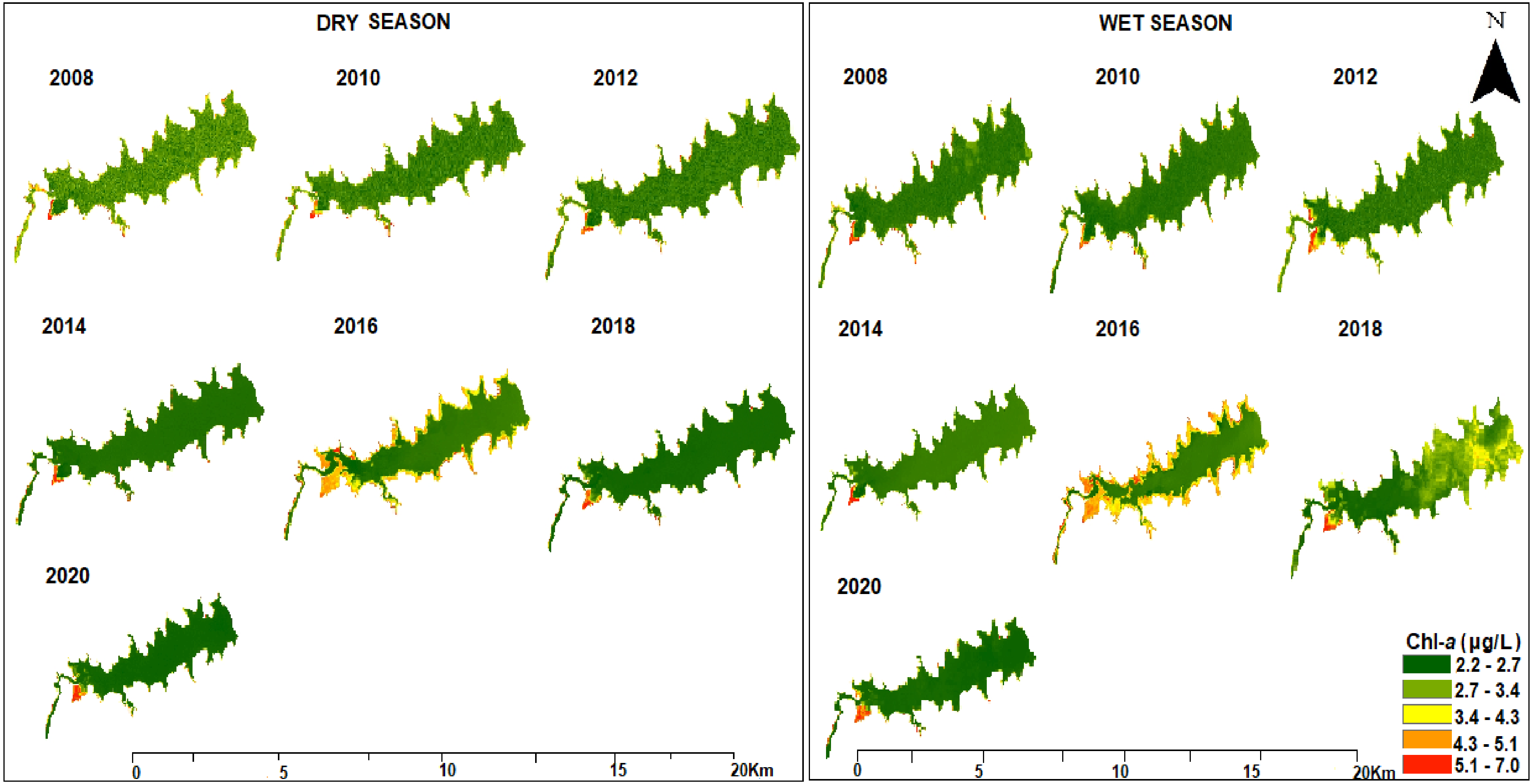

Figure 6. Distribution of chlorophyll–*a* concentration in Nandoni reservoir in Vhembe District, Limpopo province of South Africa

4.5 Relationship between in–situ and remotely sensed chlorophyll–a concentration

The estimated results of observed and predicted chl–*a* concentration of Nandoni reservoir were determined in terms of the coefficient of determination (R^2), root mean square error (RMSE) and RMSE% (Figure 7). The linear regression result showed a strong and positive association between the observed and predicted variables with the R^2 value of 0.91. The RMSE results showed a positive correlation between in–situ data and Landsat derived data with RMSE value of 0.13.

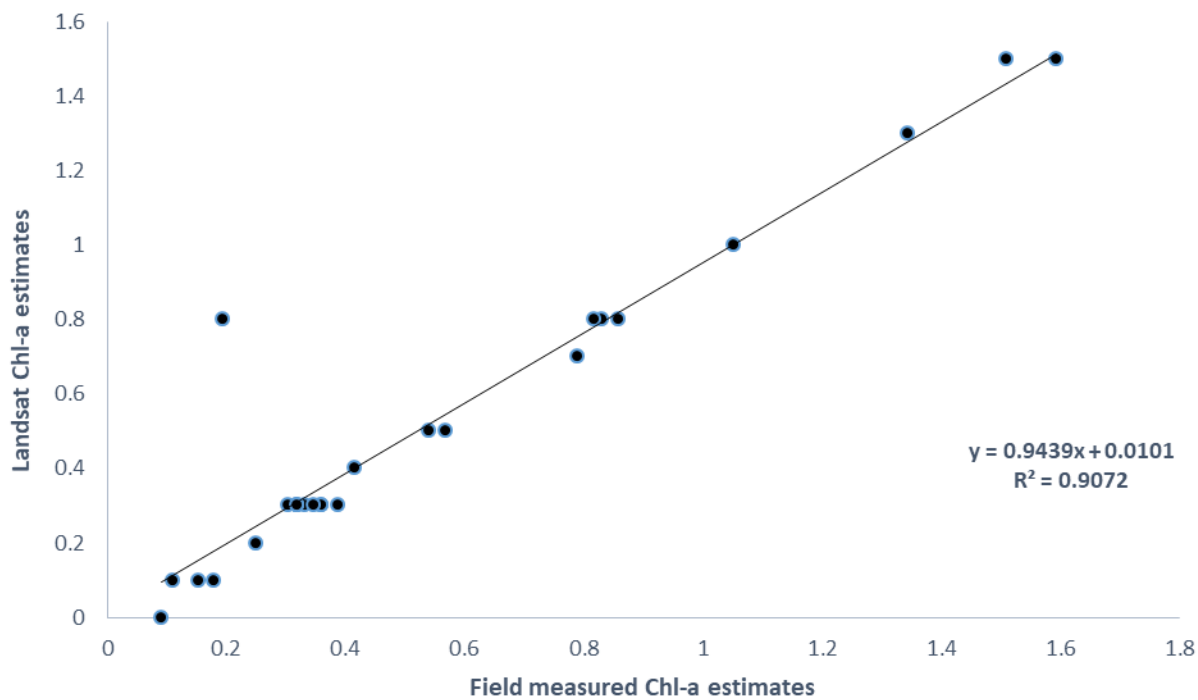

Figure 7. Landsat derived and in situ measured chl–*a* in Nandoni reservoir measured in December 2020.

CHAPTER FIVE: DISCUSSION AND CONCLUSIONS

5. Discussion

5.1 Temporal variation in physicochemical variables

The pH range of 7.3– to 9.3 indicated an acceptable range for most aquatic life. However, the suggested pH range for phytoplankton optimum growth condition is 7.4– to 8.0 (Rai and Rajashekar, 2014). The pH range in the middle reservoir zone had a higher than the suggested range suggesting an impact of anthropogenic activities on phytoplankton productivity. The temperature ranges from the study area ranged from 24.8 to 27.9 °C, within the acceptable temperature range for phytoplankton productivity ranging between 26.5 °C and 27.9 °C was recorded in the middle zone towards the dam zone, while the river zone recorded lower values of less than 26 °C. At a temperature of between 26 °C and 35 °C phytoplankton productivity tends to be successful (Robarts and Zohary 1987).

5.2 In–situ chlorophyll–*a* concentration relationship with physicochemical variables

Chl–*a* concentration values were recorded in the dam zone with values ranging from 0.10 to 1.46 μg L^{-1}. This was indicative of the effect of temperature and pH on chl–*a* concentration. Furthermore, it was evident that a positive relationship existed between temperature and pH with chl–*a* concentration. The high salinity values greater than 129.3 ppt at the middle and river zones corresponded with high TDS values from the two zones. This suggested an impact of agricultural practices along the reservoir catchment and runoff from nearby settlements lead to increased salinization of the Nandoni reservoir. Anthropogenic activities such as pesticides that are applied in agricultural fields and urban runoff account for excessive nutrients and toxicants in waterbodies

(Stensel 2004). However, TDS values from the three zones support the growth of phytoplankton and they could have had a negative impact if they were more than 1000 mg L^{-1} (Pal *et al*. 2015). The same is true about conductivity values for the middle and river zones despite the dam zone having recorded a high value of 292.4 µS cm^{-1}.

Conductivity seemed not to have affected the chl–*a* concentrations since the river and dam zones recorded a high average of 273.0 and 273.4 µS cm^{-1}, respectively but chl–*a* concentrations in the two sites differed significantly with the dam zone recording the highest conductivity values. The middle zone recorded a mean conductivity value of 268.1 µS cm^{-1} recorded higher –than the river zone. Therefore, high conductivity values seemed not to have had an impact on chl–*a* concentrations and the same can be concluded for resistivity. Therefore, it can also be argued that the decreasing chl–*a* concentrations from the dam to the river zones were positively correlated with ORP. This suggested that the chl–*a* concentration –was at acceptable values and did not affect dissolved oxygen content, hence the ORP. The ORP seemed to correspond with an increase in chl–*a* concentration suggesting that an increase in phytoplankton densities was correlated to increases in redox potential. Kunlasak *et al.* (2013) similarly noted that phytoplankton is a major source of oxygen in fishponds, but uncontrolled phytoplankton growth can become problematic to waterbodies. It can therefore be concluded that the chl–*a* concentrations –in the reservoir were of acceptable densities.

5.3 Water quality assessment based on pollutant source

Land use was studied to determine the impact of water quality in Nandoni reservoir. The present study revealed that agriculture and settlements were the main land use and land cover types closer to the reservoir. Settlements play a significant role in determining the water quality of a reservoir. Based on literature, land use within the watershed has a significant impact on the reservoir water quality and quantity (Khan *et al.* 2015; Olusola *et al*. 2018). The shoreline distance from the reservoir to the settlement that is at greater than >100 m contributes to microplastics can lead to deterioration of water quality, and it was observed that plastic pollution was more associated with domestic solids waste. Solid and liquid waste generated from the settlements along the reservoir shorelines were deposited into the reservoir, and this slowly affects water quality due to an increase in population, as the reservoir slowly purifies itself. Zhao *et al.* (2018) highlighted that all these activities can lead to increased eutrophication of the reservoir.

Recreational and construction activities closer to the reservoir contribute to the structuring of species diversity by increasing the surface runoff and soil erosion after flooding which decrease the water quality and quantity. Some community members also use the reservoir water for washing laundry and cleaning vehicles which could increase water phosphorus levels, which may result into accelerated phytoplankton growth and poor water quality that may lead into death of aquatic species and impacting the water body. These activities can affect and cause changes to physicochemical parameters such as TDS, conductivity, pH and salinity which could be due to the presence of community closer to the reservoir. Therefore, these changes may reduce water quality by encouraging rapid phytoplankton growth in the reservoir. Tollefson (2018) highlighted that high phytoplankton growth in water bodies may pose serious health risk to human and livestock.

The increased human population relies on agricultural land for their livelihood. Agriculture in the proximity of the water body contributes to high salinity and pH concentrations, due to the fertiliser transport from erosion by rainfall to the waterbody. The unsustainable agriculture methods near the reservoir also cause soil erosion and, as a result, reservoir water quality deterioration due to sedimentation. Therefore, excessive use of organic and inorganic fertilisers and veld fires may result in high nutrients and eutrophication of reservoirs. Areas used for animal grazing near the shoreline might lead to increased faecal matter finding its way into the water body through surface run off. Awtwi *et al.* (2015) highlighted that high density of grazing animals closer to a water body could also be an important source of nutrients in the system. During this study, it was observed that excessive nutrients disposal in the water body resulted into high chl–*a* concentration in a small bay of the reservoir dam zone. Gildea (2000) reported a similar trend from his study, where the watershed with high agricultural land tends to be associated with increased deposition of phosphorus and nitrogen due fertilizer application in the agricultural fields.

5.4 Remotely sensed and in situ measurements in Nandoni reservoir

The chl–*a* concentration distribution maps were estimated based on an algorithm by Wibowo *et al.* (1993), were the Red and NIR band ratio were used to retrieve chl–*a* concentration from the reservoir, showing the real potential of applying remote sensing in monitoring chl–*a* concentration in water bodies. The algorithm applied to this study showed the potential for estimating chl–*a* concentration in the water ecosystems. Classes represented on the images were retrieved from the empirical model used by Buditama *et al.* (2017). No filtering was applied on the data, therefore, Landsat 8 OLI showed higher dynamic range than Landsat ETM+ imagery. This could be attributed to the improvement of radiometric resolution and changes related to spectral response of Landsat OLI sensors (Lymburner *et al.* 2016).

Maps generated in December 2020, showed a complex spatial structure of chl–*a* with high values mainly observed in the reservoir dam zone. This could be related to the anthropogenic activities linked to Madzivhandila Agricultural College, Budeli, recreational and construction activities, animal grazing, and excessive nutrients disposal from the farms closer to the dam zone. Slight eutrophication or algal blooms was observed in the dam zone during sampling. Therefore, high chl–*a* concentration in the dam zone could be as result of improper disposal of domestic waste. Different authors (e.g., Giardino *et al*. 2010) have suggested that most algal growth are in areas affected by excessive nutrient runoff to the reservoir zones where nutrients are more concentrated. The catchment of Nandoni reservoir had settlements and agricultural activities which were closer to the dam zone which resulted in excessive nutrient load. Banansea *et al.* (2016) highlighted similar results that continuous reduction of bushland will in turn lead to an increase of human induced activities such as agriculture and residential development. In the current study, these activities have resulted into deterioration of water quality in the reservoir.

Matthews (2016) suggested that there are a large number of investigations that used Landsat sensors to assess water quality characteristics. Most of the water quality investigations employ a combination of bands and ratios, and this algorithm of chl–*a* estimates, varies from one reservoir to another. In the present study, the algorithm used to estimate chl–*a* concentration in the reservoir was applied using a combination of different bands (red, NIR) of Landsat 7 ETM+ and Landsat 8 OLI sensors. Similar results were highlighted by Tebbs *et al.* (2013) that combination bands of red and NIR of Landsat 7 ETM+ sensor were used to estimate chl–*a* in Lake Bogoria, Kenya. There was a considerable wet and dry season difference in chl–*a* concentration and primary production within Nandoni reservoir. Landsat 8 OLI showed high chl–*a* concentrations were observed in the river zone, while getting lower in the middle and dam zones. The distribution of chl–*a* varied spatially and temporally within the reservoir. It can simply be observed that during dry season in the year 2008, chl–*a* concentration was high in the river zone while low in the middle and dam zone. In the year 2010 to 2014, chl–*a* concentration was high in a small bay of the river zone and low in the middle and dam zone. Therefore, anthropogenic activities such as washing laundries, grazing animals, subsistence farming and mud brick manufacturing may account to excessive nutrients which led to phytoplankton growth in the river zone. Low chl–*a* concentration could be assigned to the dilution due to the freshwater inflow from the Luvuvhu River and the increased sediments loads which would limit primary production in the reservoir.

In year 2016, satellite sensors detected highest chl–*a* concentration was observedin wet and dry season along the shorelines of the reservoir, while getting lower in the middle and dam zone, this was due to low water capacity. Dalu *et al.* (2013) highlighted that, as water level drops, the reservoir undergoes a self–purifying process where it allows oxygen to recharge the bottom water and increase surface nutrients. During the detection of phytoplankton biomass in the reservoir, the optical classification method of water bodies revealed that, plants found in the shoreline had been detected as algae because plants also contain chlorophyll pigments. Therefore, in the year 2018 and 2020, chl–*a* concentration observed in wet and dry season was very high in a small bay in the river zone because of agricultural pesticides and population increase closer to the reservoir, where nutrients runoff was deposited in a small bay in the reservoir river zone. The observations were similar to Dalu *et al.* (2013b) who suggested that the supply of nutrients contribute to an increase in chl–*a* concentration leading to phytoplankton growth. Spatial distribution of low chl–*a* concentration persisted in the middle and dam zones in all years especially during dry season.

The chl–*a* concentration increased in the wet season compared with results obtained in dry season. In year 2008 to 2014, high chl–*a* concentration were estimated in the river zone, getting lower in the middle and dam zone. Sufficient light, temperature and nutrient availability in the surface water promotes phytoplankton growth in the reservoir resulting in high chl–*a* concentration in the water body (Dupuis and Hann 2009; Dalu *et al*. 2013b). Dalu *et al.* (2013) suggested that the availability of nutrients in lakes and reservoir are influenced by various factors including atmospheric dust particle deposition, river input, decomposition of organic matter and bottom sediment resuspension.

In year 2018, the high chl–*a* concentration were recorded in a small bay of the river zone and becoming low in a small section of the middle and dam zone. This resulted in excessive nutrients which accumulate in the shorelines from human activities, agricultural pesticides, urban runoff, and municipal sewage deposited in the water body through water runoff. These observations were similar to Ndungu *et al.* (2013) who also suggested that high reflectance of turbidity constituents such as suspended matter can affect chl–*a* concentration in water bodies as observed in year 2018.

In year 2020, chl–*a* concentration was high in a small bay in the river zone, as a result of excessive nutrients from agricultural pesticides, population increase as they play a significant role in the disposal of nutrients from the water runoff. Important factors attributed to affecting the distribution of phytoplankton biomass in deeper water of the reservoir are wind activity and river inflow. Wind activity could have contributed to high chl–*a* concentration within the littoral zone of the reservoir due to the availability of nutrients accumulated in the water column. Additionally, excessive nutrients disposal in the reservoir are responsible for phytoplankton growth. The differences in chl–*a* concentration in the same month for the different years suggests that phytoplankton development is influenced by environmental conditions as well as changes in time and space. Buttencourt *et al*. (2019) highlighted that surface water temperatures in the reservoir have the most impact on the year–to–year changes. Water temperature and suspended solids were responsible for the spatiotemporal changes of phytoplankton distribution in Nandoni reservoir. Therefore, suspended solids were detected in the river zone during the study months and years where they are most likely linked to increasing phytoplankton production. This shows there is fluctuation of chl–*a* concentration due to seasonal changes. According to Makhera *et al.* (2010), suggested that high nutrients concentration from domestic waste from Thohoyandou wastewater treatment works and agriculture may lead to phytoplankton growth which degrade the quality of surface water, and this resulted to decreased dissolve oxygen level in the water and affected aquatic plants and animals (Nas and Berktay 2006).

6. Conclusions

Based on the predicted and observed chl–*a* concentration, Nandoni reservoir was considered to have low chl–*a* concentration. The algorithm employed on satellite images to derive chl–*a* concentration worked successfully on Landsat 7 ETM+ and 8 OLI images. The resolution of Landsat 7 and 8 allowed us to successfully determine and estimate the spatio–temporal distribution of chl–*a* in Nandoni reservoir. It can also be concluded the Landsat 7 ETM+ and 8 OLI are suitable for monitoring of phytoplankton biomass in freshwater ecosystem and map where chl–*a* is abundant. It was also attested by linear regression analysis which showed high level of agreement of correlation values (R^2 = 0.91, RMSE = 0.13) between the field chl–*a* and predicted chl–*a*.

From the findings of this study, Nandoni reservoir was considered as oligotrophic system. Therefore, our findings on the relationship between chl–*a* and physicochemical variables within the reservoir have significantly improved our understanding on the influence of hydrological state of Nandoni reservoir. The results also showed that settlement and agricultural practices closer to the reservoir played a significant role on the reservoir water quality. Therefore, all physio–chemical parameters measured in this study, temperature, pH, salinity, TDS, ORP, conductivity and resistivity were suitable for domestic use and aquatic life. Based on Pearson correlation analysis, the results showed water temperature, pH, and conductivity had a positive relationship with chl–*a* concentration in Nandoni reservoir.

7. Recommendation

- There is a need to study the relationship between phytoplankton productivity and the size, structure and age of the reservoir, as this is important in determining whether reservoir characteristics have significant impact on phytoplankton production. There is less published data on this.Operational characteristics of reservoirs should be considered when measurering phytoplankton productivity. Reservoirs that are being overutilized for recreational and economic purposes need frequent observations of phytoplankton production as the changes might be significant within shorter periods.
- The use of modern technological approach such as remote sensing should be supplemented by frequent phytoplankton productivity observations since these technologies record momentary events but might miss to record those happening continuously for shorter periods.

- There is need to frequently study the correlation between plankton productivity and aquatic composition in order to explain the relationship between them and the reservoir characteristics.

REFERENCES

Abbasnia, A., Yousefi, N., Mahvi, A.H., Nabizadeh, R., Radfard, M., Yousefi, M., Alimohammadi, M., 2019. Evaluation of groundwater quality using water quality index and its suitability for assessing water for drinking and irrigation purposes: Case study of Sistan and Baluchistan province (Iran). *Human and Ecological Risk Assessment: An International Journal*, 25, 988–1005.

Almomani, F.A., Örmeci, B., 2018. Monitoring and measurement of microalgae using the first derivative of absorbance and comparison with chlorophyll extraction method. *Environmental Monitoring and Assessment*, 190, 1–19.

Allan, A., Rieu–Clarke, A., Tyagi, A.C., 2006. Legal and institutional aspects of integrated flood management. Flood Management Policy Series; APFM Technical Document; No. 2. World Meteorological Organization (WMO).

An, K.G., Kim, D.S., 2003. Response of reservoir water quality to nutrient inputs from streams and in–lake fish farms. *Water, Air, and Soil Pollution*, 149, 27–49.

Arief, M., 2017. Development of Dissolved Oxygen Concentration Extraction Model Using Landsat Data Case Study: Ringgung Coastal Waters. *International Journal of Remote Sensing and Earth Sciences*, 12, 1–12.

Aweto, K.E., 2013. Resistivity methods in hydro–geophysical investigation for groundwater in Aghalokpe, Western Niger Delta. *Global Journal of Geological Sciences*, 11, 47–55.

Ayisi, C.L., Quarshie, B. and Cobbina, S.J., 2014. Raw water quality change and cost implication; a case study of Dalun Headwork's. *International Journal of Water Resources*, 2, 16–20.

Baykal, T., Salman, S., Acikgoz, İ., 2007. The relationship between seasonal variation in phytoplankton and zooplankton densities in Hirfanlı Dam Lake (Kırşehir, Turkey). *Turkish Journal of Biology*, 30, 217–226.

Bekele, A., Downer, R.G., Wolcott, M.C., Hudnall, W.H., Moore, S.H., 2003. Comparative evaluation of spatial prediction methods in a field experiment for mapping soil potassium. *Soil Science*, 168, 15–28.

Belkhiri, L., Mouni, L., 2014. Geochemical characterization of surface water and groundwater in Soummam Basin, Algeria. *Natural Resources Research*, 23, 393–407.

Bellinger, E.G., Sigee, D.C., 2015. *Freshwater Algae: Identification, Enumeration and Use as Bioindicators*. John Wiley and Sons, London.

Berglund, J., Müren, U., Båmstedt, U., Andersson, A., 2007. Efficiency of a phytoplankton-based and a bacterial-based food web in a pelagic marine system. *Limnology and Oceanography*, 52, 121–131.

Blakey, T., Melesse, A., Hall, M.O., 2015. Supervised classification of benthic reflectance in shallow subtropical waters using a generalized pixel–based classifier across a time series. *Remote Sensing*, 7, 5098–5116.

Blondeau–Patissier, D., Gower, J.F., Dekker, A.G., Phinn, S.R., Brando, V.E., 2014. A review of ocean colour remote sensing methods and statistical techniques for the detection, mapping and analysis of phytoplankton blooms in coastal and open oceans. *Progress in Oceanography*, 123, 123–144.

Bonansea, M., Ledesma, C., Rodriguez, M.C., 2016. Assessing the impact of land use and land cover on water quality in the watershed of a reservoir. *Applied Ecology and Environmental Research*, 14, 447–456.

Bowers, D.G., Binding, C.E., Ellis, K.M., 2007. Satellite remote sensing of the geographical distribution of suspended particle size in an energetic shelf sea. *Estuarine, Coastal and Shelf Science*, 73, 457–466.

Bowes, M.J., Gozzard, E., Johnson, A.C., Scarlett, P.M., Roberts, C., Read, D.S., Armstrong, L.K., Harman, S.A., Wickham, H.D., 2012. Spatial and temporal changes in chlorophyll–a concentrations in the River Thames basin, UK: are phosphorus concentrations beginning to limit phytoplankton biomass? *Science of the Total Environment*, 426, 45–55.

Bowes, M.J., Loewenthal, M., Read, D.S., Hutchins, M.G., Prudhomme, C., Armstrong, L.K., Harman, S.A., Wickham, H.D., Gozzard, E., Carvalho, L., 2016. Identifying multiple stressor controls on phytoplankton dynamics in the River Thames (UK) using high–frequency water quality data. *Science of the Total Environment*, 569, 1489–1499.

Bowling, L.C., Zamyadi, A., Henderson, R.K., 2016. Assessment of in situ fluorometry to measure cyanobacterial presence in water bodies with diverse cyanobacterial populations. *Water Research*, 105, 22–33.

Brando, V.E., Dekker, A.G., 2003. Satellite hyperspectral remote sensing for estimating estuarine and coastal water quality. *IEEE Transactions on Geoscience and Remote Sensing,* 41, 1378–1387.

Brezonik, P., Menken, K.D., Bauer, M., 2005. Landsat–based remote sensing of lake water quality characteristics, including chlorophyll and colored dissolved organic matter (CDOM). *Lake and Reservoir Management*, 21, 373–382.

Brus, D.J. and Heuvelink, G.B., 2007. Optimization of sample patterns for universal kriging of environmental variables. *Geoderma*, *138*(1-2), pp.86-95.

Buditama, G., Damayanti, A., Pin, T.G., 2017, Identifying distribution of chlorophyll–a concentration using Landsat 8 OLI on marine waters area of Cirebon. The IOP Conference Series: Earth and Environmental Science. Volume 98,012040. IOP Publishing.

Buma, W.G., Lee, S.I., 2020. Evaluation of sentinel–2 and landsat 8 images for estimating chlorophyll–a concentrations in lake Chad, Africa. *Remote Sensing*, 12, 2437.

Butt, A., Shabbir, R., Ahmad, S.S. and Aziz, N., 2015. Land use change mapping and analysis using Remote Sensing and GIS: A case study of Simly watershed, Islamabad, Pakistan. The Egyptian Journal of Remote Sensing and Space Science, 18, pp.251-259.

Çelekli, A., Öztürk, B., Kapı, M., 2014. Relationship between phytoplankton composition and environmental variables in an artificial pond. *Algal Research, 5*, pp.37–41.

Carmignani, J.R. and Roy, A.H., 2017. Ecological impacts of winter water level drawdowns on lake littoral zones: a review. *Aquatic Sciences*, 79, 803–824.

Cha, Y., Cho, K.H., Lee, H., Kang, T., Kim, J.H., 2017. The relative importance of water temperature and residence time in predicting cyanobacteria abundance in regulated rivers. *Water Research*, 124, 11–19.

Chang, H., 2005. Spatial and temporal variations of water quality in the Han River and its tributaries, Seoul, Korea, 1993–2002. *Water, Air and Soil Pollution*, 161, 267–284.

Chang, K.W., Shen, Y., Chen, P.C., 2004. Predicting algal bloom in the Techi reservoir using Landsat TM data. *International Journal of Remote Sensing,* 25, 3411–3422.

Chawira, M., Dube, T., Gumindoga, W., 2013. Remote sensing–based water quality monitoring in Chivero and Manyame lakes of Zimbabwe. *Physics and Chemistry of the Earth, Parts A/B/C*, 66, 38–44.

Chen, Z., Hu, C., Muller–Karger, F., 2007. Monitoring turbidity in Tampa Bay using MODIS/Aqua 250–m imagery. *Remote Sensing of Environment*, 109, 207–220.

Chapin III, F.S., Matson, P.A., Vitousek, P., 2011. *Principles of Terrestrial Ecosystem Ecology*. Springer Science and Business Media, Cham.

Cloern, J.E., Foster, S.Q., Kleckner, A.E., 2014. Phytoplankton primary production in the world's estuarine–coastal ecosystems. *Biogeosciences,* 11, 2477.

Coakes, S., Steed, L., Dzidic, P., 2006. SPSS version 13.0 for windows. Milton.

Dalu, T., Thackeray, Z., Leuci, R., Clegg, B., Chari, L.D., Nhiwatiwa, T., 2013. First results on bathymetry, stratification and physicochemical limnology of a small tropical African reservoir (Malilangwe, Zimbabwe). *Water SA*, 39, 119–130.

Dalu, T., Nhiwatiwa, T., Clegg, B., 2013. Temporal variation of the plankton communities in a small tropical reservoir (Malilangwe, Zimbabwe). *Transactions of the Royal Society of South Africa*, 68, 85–96.

Dalu, T., Malesa, B., Cuthbert, R.N., 2019. Assessing factors driving the distribution and characteristics of shoreline macroplastics in a subtropical reservoir. *Science of the Total Environment*, 696, 133992.

Day, J.W., Hall, C.A.S., Kemp, W.M., Yanes–Arancibia, A., 1989. Nekton, the free–swimming consumers. In: Day, J.W. Jr., Hall, C.A.S., Kemp, W.M., Yanes–Arancibia, A. (eds) Estuarine Ecology. Wiley Interscience, New York.

Dall'Olmo, G,, Gitelson, A.A., Rundquist, D.C., Leavitt, B., Barrow, T., Holz, J.C., 2005. Assessing the potential of SeaWiFS and MODIS for estimating chlorophyll concentration in turbid productive waters using red and near–infrared bands. *Remote Sensing of the Environment*, 96, 176–187.

Dao, T.S., Cronberg, G., Nimptsch, J., Do–Hong, L.C. and Wiegand, C., 2010. Toxic cyanobacteria from Tri An Reservoir, Vietnam. *Nova Hedwigia*, 90, 433.

De Anil, K., 2003. Environmental Chemistry. 5th Edition. New Age International Publishers, New Delhli.

Dodds, W.K., Bouska, W.W., Eitzmann, J.L., Pilger, T.J., Pitts, K.L., Riley, A.J., Schloesser, J.T., Thornbrugh, D.J., 2009. Eutrophication of US freshwaters: analysis of potential economic damages. *Environmental Science Technology*, 43, 12–19.

De–Domitrovic, Y.Z., Devercelli, M., Forastier, M.E., 2014. Phytoplankton of the Paraguay and Bermejo rivers. *Advances in Limnology*, 65, 67–80.

Doxaran, D., Froidefond, J.M., Castaing, P. and Babin, M., 2009. Dynamics of the turbidity maximum zone in a macrotidal estuary (the Gironde, France): Observations from field and MODIS satellite data. *Estuarine, Coastal and Shelf Science*, 81, 321–332.

Dube, T., 2012. Primary productivity of intertidal mudflats in the Wadden Sea: a remote sensing method. Master's thesis, University of Twente, Twente.

Dube, T., Gumindoga, W., Chawira, M., 2014. Detection of land cover changes around Lake Mutirikwi, Zimbabwe, based on traditional remote sensing image classification techniques. *African Journal of Aquatic Science*, 39, 89–95.

Dube, T., Mutanga, O., Seutloali, K., Adelabu, S., Shoko, C., 2015. Water quality monitoring in sub–Saharan African lakes: a review of remote sensing applications. *African Journal of Aquatic Science*, 40, 1–7.

Ekercin, S., 2007. Water quality retrievals from high resolution IKONOS multispectral imagery: A case study in Istanbul, Turkey. *Water, Air, and Soil Pollution*, 183, 239– 251.

El–Serehy, H.A., Abdallah, H.S., Al–Misned, F.A., Irshad, R., Al–Farraj, S.A., Almalki, E.S., 2018. Aquatic ecosystem health and trophic status classification of the Bitter Lakes along the main connecting link between the Red Sea and the Mediterranean. *Saudi Journal of Biological Sciences*, 25, 204–212.

ESRI., 2015. ArcGIS 10.5: Using ArcGIS Spatial Analyst. Software User Guide ESRI, USA

Finn, M.P., Reed, M.D., Yamamoto, K.H., 2012. A straightforward guide for processing radiance and reflectance for EO–1 ALI, Landsat 5 TM, Landsat 7 ETM+, and ASTER. Unpublished Report from USGS/Center of Excellence for Geospatial Information Science.

Franz, B.A., Bailey, S.W., Kuring, N., Werdell, P.J., 2015. Ocean color measurements with the Operational Land Imager on Landsat–8: implementation and evaluation in SeaDAS. *Journal of Applied Remote Sensing*, 9, 096070.

Freeman, L.A., Corbett, D.R., Fitzgerald, A.M., Lemley, D.A., Quigg, A., Steppe, C.N., 2019. Impacts of urbanization and development on estuarine ecosystems and water quality. *Estuaries and Coasts*, 42, 1821–1838.

Gholizadeh, M.H., Melesse, A.M., Reddi, L., 2016. A comprehensive review on water quality parameters estimation using remote sensing techniques. *Sensors*, 16, 1298.

Giardino, C., Bresciani, M., Villa, P., Martinelli, A., 2010. Application of remote sensing in water resource management: the case study of Lake Trasimeno, Italy. *Water Resources Management*, 24, 3885–3899.

Gin, K.Y.H., Koh, S.T., Lin, I.I., Chan, E.S., 2002. Application of spectral signatures and colour ratios to estimate chlorophyll in Singapore's coastal waters. *Estuarine, Coastal and Shelf Science*, 55, 719–728.

Gitelson, A.A., Schalles, J.F.. Hladik, C.M., 2007. Remote chlorophyll–a retrieval in turbid, productive estuaries: Chesapeake Bay case study. *Remote Sensing of Environment*, 109, 464–472.

Gitelson, A.A., Dall'Olmo, G., Moses, W., Rundquist, D.C., Barrow, T., Fisher, T.R., Gurlin, D., Holz, J., 2008. A simple semi–analytical model for remote estimation of chlorophyll–a in turbid waters: Validation. *Remote Sensing of Environment*, 112, 3582–3593.

Gitelson, A.A., Yacobi, Y.Z., Karnieli, A., Kress, N., 1996. Reflectance spectra of polluted marine waters in Haifa Bay, Southeastern Mediterranean: Features and application for remote estimation of chlorophyll concentration. *Israel Journal of Earth Sciences*, 45, 127–136.

Gons, H.J., Auer, M.T., Effler, S.W., 2008. MERIS satellite chlorophyll mapping of oligotrophic and eutrophic waters in the Laurentian Great Lakes. *Remote Sensing of Environment*, 112, 4098–4106.

Guettaf, M., Maoui, A., Ihdene, Z., 2017. Assessment of water quality: a case study of the Seybouse River (North–East of Algeria). *Applied Water Science*, 7, 295–307.

Gurung, T.B., Dhakal, R.P., Bista, J.D., 2006. Phytoplankton primary production, chlorophyll-a and nutrient concentrations in the water column of mountainous Lake Phewa, Nepal. *Lakes and Reservoirs: Research and Management*, 11, 141–148.

Gregor, J., Maršálek, B., 2004. Freshwater phytoplankton quantification by chlorophyll a: a comparative study of in vitro, in vivo and in situ methods. *Water Research*, 38, 517–522.

Haliuc, A., Buczkó, K., Hutchinson, S.M., Ács, É., Magyari, E.K., Korponai, J., Begy, R.C., Vasilache, D., Zak, M., Veres, D., 2020. Climate and land–use as the main drivers of recent environmental change in a mid–altitude mountain lake, Romanian Carpathians. *PloS One*, 15, e0239209.

Halpern, B.S., Walbridge, S., Selkoe, K.A., Kappel, C.V., Micheli, F., D'Agrosa, C., Bruno, J.F., Casey, K.S., Ebert, C., Fox, H.E., Fujita, R., 2008. A global map of human impact on marine ecosystems. *Science*, 319, 948–952.Han, L., Rundquist, D.C., 1997. Comparison of NIR/RED ratio and first derivative of reflectance in estimating algal–chlorophyll concentration: a case study in a turbid reservoir. *Remote Sensing of the Environment*, 62, 253–261.

Han, L., Jordan, K.J., 2005. Estimating and mapping chlorophyll-a concentration in Pensacola Bay, Florida using Landsat ETM+ data. *International Journal of Remote Sensing,* 26, 5245–5254.

Han, L., Rundquist, D.C., 1997. Comparison of NIR/RED ratio and first derivative of reflectance in estimating algal–chlorophyll concentration: A case study in a turbid reservoir. *Remote sensing of Environment*, 62, 253–261.

Hansen, M.C. and Loveland, T.R., 2012. A review of large area monitoring of land cover change using Landsat data. Remote sensing of Environment, 122, 66-74.

Harvey, E.T., Kratzer, S., Philipson, P., 2015. Satellite–based water quality monitoring for improved spatial and temporal retrieval of chlorophyll–a in coastal waters. *Remote Sensing of Environment*, 158, 417–430.

Heaney, M.B., 2003. Electrical conductivity and resistivity. In: Webster, J.G. (ed) *Electrical Measurement, Signal Processing, and Displays*. CRC Press, London.

International Lake Environment Committee, 1999. Guidelines of Lake Management. Volume 9: Reservoir Water Quality Management. United Nations Environment Programme; International Lake Environment Committee, Tokyo.

Intergovernmental Panel on Climate Change (IPCC)., 2007. Climate Change: Impacts, Adaptation and Vulnerability. Contribution of Working Group II to the Fourth Assessment Report of the Intergovernmental Panel on Climate Change. Cambridge University Press, Cambridge.

Isari, S., Antó, M., Saiz, E., 2013. Copepod foraging on the basis of food nutritional quality: can copepods really choose. *PloS One*, 8, e84742.

ISO 5667–4: 1987 Water quality—Sampling—Part 4: Guidance on sampling from lakes,

natural and man–made.Jensen, J.R., Hodgson, M.E., Tullis, J.A., Raber, G.T., 2005. Remote sensing of impervious surfaces and building infrastructure. In: Jensen, R.R., Gatrell, J.D., McLean, D.D. (eds) *Geo–Spatial Technologies in Urban Environments.* Springer, Berlin.

Jensen, J.R., Hodgson, M.E., Tullis, J.A., Raber, G.T., 2005. Remote sensing of impervious surfaces and building infrastructure. In: Jensen, R.R., Gatrell, J.D., McLean, D.D. (eds) *Geo–Spatial Technologies in Urban Environments.* Springer, Berlin.

Jeppesen, E., Meerhoff, M., Davidson, T.A., Trolle, D., Sondergaar, D., M., Lauridsen, T.L., Beklioglu, M., Brucet Balmaña, S., Volta, P., González–Bergonzoni, I., Nielsen, A., 2014. Climate change impacts on lakes: an integrated ecological perspective based on a multi–faceted approach, with special focus on shallow lakes. *Journal of Limnology*, 73, 84–107

Jeppesen, E., Brucet, S., Naselli–Flores, L., Papastergiadou, E., Stefanidis, K., Noges, T., Noges, P., Attayde, J.L., Zohary, T., Coppens, J., Bucak, T., 2015. Ecological impacts of global warming and water abstraction on lakes and reservoirs due to changes in water level and related changes in salinity. *Hydrobiologia*, 750, 201–227.

Juahir, H., Zain, S.M., Yusoff, M.K., Hanidza, T.T., Armi, A.M., Toriman, M.E., Mokhtar, M., 2011. Spatial water quality assessment of Langat River Basin (Malaysia) using environmetric techniques. *Environmental Monitoring and Assessment*, 173, 625–641.

Karamouz, M., Szidarovszky, F. and Zahraie, B., 2003. *Water Resources Systems Analysis*. CRC Press, London.

Kenderov, L., Pavlova, M., Trichkova, T., Tyufekchieva, V., Vidinova, Y., Kozuharov, D., Botev, I., Hubenov, Z., Uzunov, Y., Stoichev, S., Beshkova, M., 2014. Trophic state and trophic structure in three Bulgarian reservoirs. *Acta Zoologica Bulgarica*, 66, 247–254.

Kazi, T.G., Arain, M.B., Jamali, M.K., Jalbani, N., Afridi, H.I., Sarfraz, R.A., Baig, J.A., Shah, A.Q., 2009. Assessment of water quality of polluted lake using multivariate statistical techniques: A case study. *Ecotoxicology and Environmental Safety*, 72, 301–309.

Khattab, M.F., Merkel, B.J., 2014. Application of Landsat 5 and Landsat 7 images data for water quality mapping in Mosul Dam Lake, Northern Iraq. *Arabian Journal of Geosciences*, 7, 3557–3573.

Kimmel, B. L., Lind, O.T., Paulson, L.J., 1990. Reservoir primary production. In: Thornton, K.W., Kimmel, B.L., Payne, F.E. (eds), *Reservoir Limnology: Ecological Perspectives*. John Wiley and Sons, New York.

Kirk, J.T., 1994. Light and Photosynthesis in Aquatic Ecosystems. Cambridge University Press, Cambridge.

Kuang, Q., Bi, Y., Zhou, G., Cai, Q., Hu, Z., 2005. Study on the phytoplankton in the Three Gorges Reservoir before and after sluice and the protection of water quality. *Acta Hydrobiologica Sinica*, 29, 358.

Kunlasak, K., Chitmanat, C., Whangchai, N., Promya, J., Lebel, L., 2013. Relationships of dissolved oxygen with chlorophyll–a and phytoplankton composition in tilapia ponds. *International Journal of Geosciences*, 4, 46.

Laslett, G.M., McBratney, A.B., Pahl, P. and Hutchinson, M.F., 1987. Comparison of several spatial prediction methods for soil pH. *Journal of Soil Science, 38*(2), pp.325–341.

Lavery, P., Pattiaratchi, C., Wyllie, A., Hick, P., 1993. Water quality monitoring in estuarine waters using the Landsat Thematic Mapper. *Remote Sensing of Environment*, 46, 268–280.

Lerdburoos, Y., Tarnchalanukit, W., Tabthipwon, P., Yoonphand, R., 2013. Relationship among nutrients, chlorophyll–a, physical and chemical properties of water in Srinadharin Reservoir, Kanchanaburi Province. *Naresuan University Journal: Science and Technology*, 18, 9–16.

Lehman, J.T., 2014. Understanding the role of induced mixing for management of nuisance algal blooms in an urbanized reservoir. *Lake Reservoir Management*, 30, 63–71.

Li, Q., Xiao, J., Ou, T., Han, M., Wang, J., Chen, J., Li, Y., Salmaso, N., 2018. Impact of water level fluctuations on the development of phytoplankton in a large subtropical reservoir: implications for the management of cyanobacteria. *Environmental Science and Pollution Research*, 25, 1306–1318.

Li, C., Feng, W., Chen, H., Li, X., Song, F., Guo, W., Giesy, J.P., Sun, F., 2019. Temporal variation in zooplankton and phytoplankton community species composition and the affecting factors in Lake Taihu—a large freshwater lake in China*. Environmental Pollution*, 245, 1050–1057.

Li, R., Li, J., 2004. Satellite remote sensing technology for lake water clarity monitoring: an overview. *Environmental Informatics Archives*, 2, 893–901.

Lillesand, T.M., 2002, Combining satellite remote sensing and volunteer Secchi disk measurement for lake transparency monitoring. Proceedings: National Monitoring Conference, National Water Quality Monitoring Council . University of Wisconsin, Madison, WI.

Lim, W.Y., Aris, A.Z., Praveena, S.M., 2013. Application of the chemometric approach to evaluate the spatial variation of water chemistry and the identification of the sources of pollution in Langat River, Malaysia. *Arabian Journal of Geosciences*, 6, 4891–4901.

Longley, P.A., Goodchild, M.F., Maguire, D.J., Rhind, D.W., 2005. *Geographic Information Systems and Science*. John Wiley and Sons, London.

Lymburner, L., Botha, E., Hestir, E., Anstee, J., Sagar, S., Dekker, A., Malthus, T., 2016. Landsat 8: Providing continuity and increased precision for measuring multi–decadal time series of total suspended matter. *Remote Sensing of Environment*, 185, 108–118.

McGrane, S.J., 2016. Impacts of urbanisation on hydrological and water quality dynamics, and urban water management: a review. *Hydrological Sciences Journal*, 61, 2295–2311.

Mahmud, A. and Achide, A.S., 2012. Analysis of land use/land cover changes to monitor urban sprawl in Keffi-Nigeria. Environmental Research Journal, 6, 129-134.

Margalef, R., 1958. Temporal succession and spatial heterogeneity. In; Buzzati-Traverso, A.A. (ed) Perspectives in Marine Biology. University of California Press, Los Angeles.

Matthews, M.W., Bernard, S., Winter, K., 2010. Remote sensing of cyanobacteria–dominant algal blooms and water quality parameters in Zeekoevlei, a small hypertrophic lake, using MERIS. *Remote Sensing Environment*, 114, 2070–2087.

Moura, A.N., Severiano, J.S., Tavares, N.K.A., Dantas, E.W., 2013. The role of a cascade of reservoirs and seasonal variation in the phytoplankton structure in a tropical river. Brazilian *Journal of Biology*, 73, 291–298.

McNeely, R.N., Neimanis, V.P., Dwyer, L., 1979. Water quality sourcebook: A guide to water quality parameters. Environment Canada, Inland Waters Directorate. Water Quality Branch, Ottawa.

Mehta, K.V., 2010. Physicochemical characteristics and statistical study of groundwater of some places of Vadgam taluka in Banaskantha district of Gujarat state (India). *Journal of Chemical and Pharmaceutical Research*, 2, 663–670.

Meier, S., Soininen, J., 2014. Phytoplankton metacommunity structure in subarctic rock pools. *Aquatic Microbial Ecology*, 73, 81–91.

Mélin, F., Sclep, G., 2015. Band shifting for ocean color multi–spectral reflectance data. *Optics Express*, 23, 2262–2279.

Mittenzwey, K.H., Ullrich, S., Gitelson, A.A., Kondratiev, K.Y., 1992. Determination of chlorophyll a of inland waters on the basis of spectral reflectance. *Limnology and Oceanography*, 37, 147–149.

Moses, W.J., Gitelson, A.A., Berdnikov, S., Povazhnyy, V., 2009. Estimation of chlorophyll–a concentration in case II waters using MODIS and MERIS data—successes and challenges. *Environmental Research Letters*, 4, 045005.

Mouquet, N., Loreau, M., 2003. Community patterns in source–sink metacommunities. *The American Naturalist*, 162, 544–557.

Murphy, R.R., Curriero, F.C., Ball, W.P., 2010. Comparison of spatial interpolation methods for water quality evaluation in the Chesapeake Bay. *Journal of Environmental Engineering*, 136, 160–171.

Nair, G.A., Mohamed, A.I., Premkumar, K., 2005. Physico chemical parameters and correlation coefficients of ground waters of north–east Libya. *Pollution Research*, 24, 1.

Nair, A., Sathyendranath, S., Platt, T., Morales, J., Stuart, V., Forget, M.H., 2008. Remote sensing of phytoplankton functional types. *Remote Sensing of Environment*, 112, 3366–3375.

Nas, B., Berktay, A., 2006. Groundwater contamination by nitrates in the city of Konya, (Turkey): A GIS perspective. *Journal of Environmental Management*, 79, 30–37.

Nazari–Zade, F., Arshadiyan, F., Zand–Vakily, K., 2006. Study of spatial variability of Groundwater quality of Balarood Plain in Khuzestan province. Proceedings of the first congress of optimized exploitation from water source of Karoon and Zayanderood Plain. Shahrekord University, Shahrekord.

Neisi, A., Mirzabeygi, M., Zeyduni, G., 2018. Data on fluoride concentration levels in cold and warm season in City area of Sistan and Baluchistan Province, Iran. *Data Brief*, 18, 713–718.

O'Boyle, S., McDermott, G., Silke, J., Cusack, C., 2016. Potential impact of an exceptional bloom of Karenia mikimotoi on dissolved oxygen levels in waters off western Ireland. *Harmful Algae*, 53, 77–85. Olmanson, L.G., Brezonik, P.L., Bauer, M.E., 2015. Remote sensing for regional lake water quality assessment: capabilities and limitations of current and upcoming satellite systems. In: Younos, T., Parece, T.E. (eds) *Advances in Watershed Science and Assessment*. Springer, Cham.

Östlund, C., Flink, P., Strömbeck, N., Pierson, D., Lindell, T., 2001. Mapping of the water quality of Lake Erken, Sweden, from imaging spectrometry and Landsat Thematic Mapper. *Science of the Total Environment*, 268, 139–154.

Ozesmi, S.L. and Bauer, M.E., 2002. Satellite remote sensing of wetlands. *Wetlands Ecology and Management*, 10, 381–402.

Pahlevan, N., Lee, Z., Wei, J., Schaaf, C.B., Schott, J.R., Berk, A., 2014. On–orbit radiometric characterization of OLI (Landsat–8) for applications in aquatic remote sensing. *Remote Sensing of Environment*, 154, 272–284.

Pal, M., Samal, N.R., Roy, P.K., Roy, M.B., 2015. Electrical conductivity of lake water as environmental monitoring–A case study of Rudrasagar Lake. *IOSR Journal of Environmental Sciences, Toxicology, Food Technology*, 9, 66–71.

Paulette, A.M., Allassane, O., Germain, G., 2011. Seasonal variation in the diversity and abundance of phytoplankton in a small African tropical reservoir. *African Journal of Microbiology Research*, 5, 2616–2626.

Petus, C., Marieu, V., Novoa, S., Chust, G., Bruneau, N., Froidefond, J.M., 2014. Monitoring spatio–temporal variability of the Adour River turbid plume (Bay of Biscay, France) with MODIS 250–m imagery. *Continental Shelf Research*, 74, 35–49.

Pringle, M.J., Schmidt, M., Muir, J.S., 2009. Geostatistical interpolation of SLC–off Landsat ETM+ images. *ISPRS Journal of Photogrammetry and Remote Sensing*, 64, 654–664.

Rangel, L.M., Silva, L.H., Rosa, P., Roland, F., Huszar, V.L., 2012. Phytoplankton biomass is mainly controlled by hydrology and phosphorus concentrations in tropical hydroelectric reservoirs. *Hydro–biological*, 693, 13–28.

Rawat, J.S., Kumar, M., 2015. Monitoring land use/cover change using remote sensing and GIS techniques: A case study of Hawalbagh block, district Almora, Uttarakhand, India. *The Egyptian Journal of Remote Sensing and Space Science*, 18, 77–84.

Reinbothe, S., Reinbothe, C., 1996. The regulation of enzymes involved in chlorophyll biosynthesis. *European Journal of Biochemistry*, 237, 323–343.

Ritchie, J.C., Rango, A., 1996. Remote sensing applications to hydrology: introduction. *Hydrological Sciences Journal*, 41, 429–431.

Robinson, T.P., Metternicht, G., 2006. Testing the performance of spatial interpolation techniques for mapping soil properties. *Computers and Electronics in Agriculture*, 50, 97–108.

Rodriguez–Lopez, L., Duran–Llacer, I., Gonzalez–Rodriguez, L., Abarca–del–Rio, R., Cardenas, R., Parra, O., Martinez–Retureta, R., Urrutia, R., 2020. Spectral analysis using LANDSAT images to monitor the chlorophyll–a concentration in Lake Laja in Chile. *Ecological Informatics*, 60, 101183.

Roelke, D., Buyukates, Y., Williams, M., Jean, J., 2004. Interannual variability in the seasonal plankton succession of a shallow, warm-water lake. *Hydrobiologia*, 513, 205–218. Roy, D.P., Wulder, M.A., Loveland, T.R., Woodcock, C.E., Allen, R.G., Anderson, M.C., Helder, D., Irons, J.R., Johnson, D.M., Kennedy, R., Scambos, T.A., 2014. Landsat–8: Science and product vision for terrestrial global change research. *Remote sensing of Environment*, 145, 154–172.

Salmaso, N., Naselli-Flores, L., Padisak, J., 2015. Functional classifications and their application in phytoplankton ecology. *Freshwater Biology*, 60, 603–619.

Sapna, K., Thangavelu, A., Mithran, S., Shanthi, K., 2018. Spatial analysis of river water quality using inverse distance weighted interpolation in Noyyal watershed in Coimbatore, Tamilnadu, India. *Research Journal of Life Sciences, Bioinformatics, Pharmaceutical and Chemical Sciences*, 4, 150.

Scavotto, R.E., Dziallas, C., Bentzon-Tilia, M., Riemann, L., Moisander, P.H., 2015. Nitrogen-fixing bacteria associated with copepods in coastal waters of the North Atlantic Ocean. *Environmental Microbiology*, 17, 3754–3765.

Schloeder, C.A., Zimmerman, N.E., Jacobs, M.J., 2001. Comparison of methods for interpolating soil properties using limited data. *Soil Science society of America Journal*, 65, 470–479.

Shen, S., Leptoukh, G.G., Acker, J.G., Yu, Z., Kempler, S.J., 2008. Seasonal variations of chlorophyll–*a* concentration in the northern South China Sea. *Geoscience and Remote Sensing Letters*, 5, 315–319.

Sigman, D.M., Hain, M.P., 2012. The biological productivity of the ocean. *Nature Education Knowledge*, 3, 1–16.

Smith, V.H., Joye, S.B., Howarth, R.W., 2006. Eutrophication of freshwater and marine ecosystems. *Limnology and Oceanography*, 51, 351–355.

Smith, J.L., Boyer, G.L., Zimba, P.V., 2008. A review of cyanobacterial odorous and bioactive metabolites: impacts and management alternatives in aquaculture. *Aquaculture*, 280, 5–20.

Souza, D.G., Bueno, N.C., Bortolini, J.C., Rodrigues, L.C., Bovo–Scomparin, V.M., de Souza Franco, G.M., 2016. Phytoplankton functional groups in a subtropical Brazilian reservoir: responses to impoundment. *Hydrobiologia*, 779, 47–57.

Supp, S.R., Ernest, S.M., 2014. Species-level and community-level responses to disturbance: a cross-community analysis. *Ecology*, 95, 1717–1723.

Tanjeck, A.E., 2019. Using multispectral remote sensing for mapping and monitoring water quality at the Vaal dam. PhD thesis.

Tebbs, E.J., Remedios, J.J., Harper, D.M., 2013. Remote sensing of chlorophyll–a as a measure of cyanobacterial biomass in Lake Bogoria, a hypertrophic, saline–alkaline, flamingo lake, using Landsat ETM+. *Remote Sensing of Environment*, 135, 92–106.

Thenkabail, P.S., Enclona, E.A., Ashton, M.S., Legg, C., De Dieu, M.J., 2004. Hyperion, IKONOS, ALI, and ETM+ sensors in the study of African rainforests. *Remote Sensing of Environment*, 90, 23–43.

Tijare, R.V., Telkhade, P.M., 2015. Role of nutrients and aquatic vegetation in eutrophication and succession of water bodies. *International Journal of Research in Biosciences, Agriculture and Technology*, 3, 362–365.

Tollefson, J., 2012. Heatwaves blamed on global warming. *Nature*, 488, 143.

Toporowska, M., Ferencz, B., Dawidek, J., 2018. Impact of lake-catchment processes on phytoplankton community structure in temperate shallow lakes. *Ecohydrology*, 11, e2017.

Torbick, N., Hu, F., Zhang, J., Qi, J., Zhang, H., Becker, B., 2008. Mapping chlorophyll–a concentrations in West Lake, China using Landsat 7 ETM+. *Journal of Great Lakes Research*, 34, 559–565.

Vaidya, S., Dhilipkumar, R., Swain, K.K., Prabhakar, V.M., Basu, A.K., 2007. Factors influencing primary productivity in Panshet and Ujjani Reservoirs, India. *Lakes and Reservoirs: Research and Management*, 12, 203–208.

USGS NASA. 2003. Preliminary assessment of the value of Landsat 7 ETM+ data following scan line corrector malfunction.Available from www.ga.gov.au/servlet.

Ushie, F.A., 2001. Formation water resistivity (Rw) determination: the SP method. *Journal of Applied Sciences and Environmental Management*, 5, 25–28.

Verma, S.R., Sharma, P., Tyagi, A., Rani, S. Gupta, A.K., Dalela, RG., 1984. Pollution and Saprobic status of eastern Kalinadi. *Limnologica*, 15, 69–133.

Vincent, R.K., Qin, X., McKay, R.M.L., Miner, J., Czajkowski, K., Savino, J., Bridgeman, T., 2004. Phycocyanin detection from LANDSAT TM data for mapping cyanobacterial blooms in Lake Erie. *Remote Sensing of Environment*, 89, 381–392.

Wang, Y., Xia, H., Fu, J., Sheng, G., 2004. Water quality change in reservoirs of Shenzhen, China: detection using LANDSAT/TM data. *Science of the Total Environment*, 328, 195–206.

Wang, F., Han, L., Kung, H.T., Van Arsdale, R.B., 2006. Applications of Landsat-5 TM imagery in assessing and mapping water quality in Reelfoot Lake, Tennessee. *International Journal of Remote Sensing*, 27, 5269–5283.

Warsa, A., Soewardi, K., Hariyadi, S., Haryadi, J., 2016. Fish community structure and trophic level at Jatigede Reservoirs Area Pre–Inundation, Sumedang District West Java. *Balitbang Journal*, 8, 29–36.

Waylett, A.J., Hutchins, M.G., Johnson, A.C., Bowes, M.J., Loewenthal, M., 2013. Physico–chemical factors alone cannot simulate phytoplankton behaviour in a lowland river. *Journal of Hydrology*, 497, 223–233.

Wu, N., Schmalz, B., Fohrer, N., 2011. Distribution of phytoplankton in a German lowland river in relation to environmental factors. *Journal of Plankton Research*, 33, 807–820.

Yang, M.D., Sykes, R.M., Merry, C.J., 2000. Estimation of algal biological parameters using water quality modelling and SPOT satellite data. *Ecological Modelling*, 125, 1–13.

Yen, T.T.H., Thai, T.T., Van Tu, N., Quang, N.X., Luu, P.T., 2021. Environmental Factors Influencing Chlorophyll–a Concentration in Tri An Reservoir, Vietnam. *VNU Journal of Science: Earth and Environmental Sciences*, 37, 13–23.

Zogo, D., 2010. Study of the Elimination of Iron and Manganese at the Time of the Potabilisation of the Water of a Dam in the Course of Eutrophication: Case of Okpara at Parakou in Benin. PhD Thesis, University of Abomey–Calavi, Abomey–Calavi.